THE ROLE OF SURFACE PROPERTIES ON THE PHYSICAL ATTRIBUTES AND STABILITY OF COCOA POWDER SYSTEMS

by

Hector Lozano Perez

A Thesis

Submitted to the Faculty of Purdue University

In Partial Fulfillment of the Requirements for the degree of

Master of Science in Agricultural and Biological Engineering

School of Agricultural and Biological Engineering

West Lafayette, Indiana

August 2020

THE PURDUE UNIVERSITY GRADUATE SCHOOL
STATEMENT OF COMMITTEE APPROVAL

Dr. Teresa Carvajal, Chair

School of Agricultural and Biological Engineering

Dr. Kingsly Ambrose

School of Agricultural and Biological Engineering

Dr. Rodolfo Pinal

Department of Industrial and Physical Pharmacy

Approved by:

Dr. Nathan Mosier

To my mother and my twin-brother, who taught the importance of education.

ACKNOWLEDGMENTS

TABLE OF CONTENTS

LIST OF TABLES

LIST OF FIGURES

LIST OF ABBREVIATIONS

ANOVA   Analysis of variance

CfP   Cacao for Peace

CP   Cocoa Powder

°C   Celsius

DSC   Differential Scanning Calorimetry

E_{a-d} Arrhenius activation energy of diffusion

FE   Flow energy

K   Kelvin

IGC   Inverse Gas Chromatography

p   probability value

POP   1,3-dipalmitoyl-2-oleoyl-glycerol

POS   1,3-Palmitoyl-stearoyl-2-oleoyl-glycerol

R.H   Relative Humidity

SEM   Scanning Electron Microscope

sccm   Standard cubic centimeters per minute

S.D   Standard Deviation

SOS   1,3-distearoyl-2-oleoyl-glycerol

Tg   Glass transition temperature

XPS   X-Ray photoelectron spectroscopy

ABSTRACT

Cocoa is widely used by confectionary industries as a powder raw material for chocolate production. The chemical properties such as high- or low-fat content determine the functionality of the cocoa powder and constitute as a major factor in controlling the behavior of the final product. Additionally, the physicochemical properties such as the cohesive characteristics of cocoa powders create undesirable issues in industrial manufacturing settings. Thus, the evaluation of physical and chemical attributes is relevant to differentiate the powder surface structure and define the material behavior in presence of other materials or distinct environments.

This work evaluated three kinds of cocoa powders—varying mainly on the lipid content— to assess the powder performance in terms of the role of surface properties on the physical attributes (flowability and wettability) and stability under distinct frameworks. Various analytical tools were used, and several methodologies were developed and implemented to determine the surface area, changes in lipid melting phases at the surface level and particle interactions. The characterization methods included particle true density, flow properties under aerated conditions, bulk permeability, thermal properties, surface energetics, water sorption, and chemical surface compositional analyses.

The findings of this work revealed that the cocoa surface composition, amount of lipids, did not explain the low-flow performance or the water uptake. On the other hand, physicochemical properties such as lipid polymorphism was introduced as an avenue to further understand the results. From the surface energetics standpoint, a water diffusion mechanism is proposed as a result of the observed effect of water on the performance and stability of the cocoa powder systems. Owing to the hydrophobic nature of cocoa particles, this material can be used as a unique reference to understand cohesive particle models with implications on the performance (flowability and wettability) of lipid-based surface materials. The results indicated that powder behavior on the performance is a confounding effect of all variables.

The major contribution of this thesis work demonstrates the importance of surface chemistry characterization on the physical attributes of cocoa powder systems and the potential to control surface composition to improve the performance and stability of food complex systems.

1. INTRODUCTION

1.1 Cacao

The cocoa tree, *Theobroma cacao*, is mostly cultivated in the tropical regions and produces a wide range of cocoa beans that are consumed globally from their unprocessed form to processed products. Criollo, Forastero, and Trinitario are the most common genetic varieties of cocoa beans available in the market (Beg et al., 2017; Ascrizzi et al., 2017). For clarity, all products of the *Theobroma cacao* tree are referred to as cocoa, such as cocoa cake and cocoa butter.

Nowadays, cacao harvesting and the final production process involve a multistep value chain. The fruitage of cacao beans has expanded the commercialization of this business in the last 50 years. Furthermore, the consolidation of cocoa products manufacturers has occurred not only in the existing chocolate production establishments, but also in countries where the cacao fruit is harvested. Cocoa-based products have a prominent place in the market and in people's daily lives, with chocolate bars being the most widely consumed solid cocoa product (Dand, 2011).

1.1.1 Global Importance

In economic terms, cocoa powder is classified as a commodity, and a total of 3.6 million tons of cocoa powder is processed annually worldwide (Dand, 2011). The bean grinding process is conducted by multinational companies such as Cargill, Archer Daniels Midland, Barry Callebaut, Petra Foods, Blommer, and Nestlé. In Colombia, Nutresa and CasaLuker are two of the most prestigious companies where beans are processed to final products (Abbott et al. 2018).

The global demand for cocoa has experienced a growth of more than 91% between 1997 and 2017 mainly because the global supply was facilitated by a production rise of 337% and 894% from regions of Asia and Africa, respectively (Recanati et al., 2018). Cocoa exports mainly include beans and processed products such as cocoa powder, cocoa butter, cocoa cake, and cocoa liquor (Mujica et al., 2019). The major cocoa importing countries, which have the most considerable

scale of processing cocoa powder and its derivatives, are the Netherlands, the United States, and Germany; these regions consume 90% of the cocoa butter, 77% of the cocoa powder, and 88% of the cocoa liquor in the world (Dand, 2011).

1.1.2   Industrial Processing

The production of cocoa powder is subjected to different unit-level operations to obtain the desired final product with satisfactory properties. The post-harvest processing involves fermentation, drying, cleaning, crushing, roasting, milling, pressing, alkalinization, and packing of cocoa (Perego et al., 2004). Each of these unit operations must be controlled to achieve the desired organoleptic and functional properties in the final product. Figure 1.1 summarizes the unit operations involved in the conversion of cocoa fruit to cocoa powder.

The modification of the roasting process of cocoa fruit pods introduces variations in the content of methylpirazines, which are the essential molecules that provide aroma and sweetness to cocoa products. In addition, the Maillard reaction produces fluctuations in the volatile aroma-active compounds; this is attributable to the roasting process temperature that ranges between 110–140 °C (Perego et al., 2004). The polyphenolic and methylxanthine compounds present in cocoa confer pharmacological properties to the human body: flavonoids affect the cardiovascular system, and theobromine alters the nervous system (Bruinsma & Taren, 1999; Steinberg et al., 2003). The alkalinization stage alters the solubility, flavor, and color of the cocoa powder. Basically, the cocoa powder is subjected to a washing step by mixing it with an alkali solution to achieve improved physicochemical and sensory properties (Beg et al., 2017). The oxidation of polyphenols and antioxidants under the alkalinization treatment results in an improvement in consumer perception qualities (Giacometti et al., 2015). After these various treatments on the cocoa fruit pods, the roasted cocoa beans are ready for further processing.
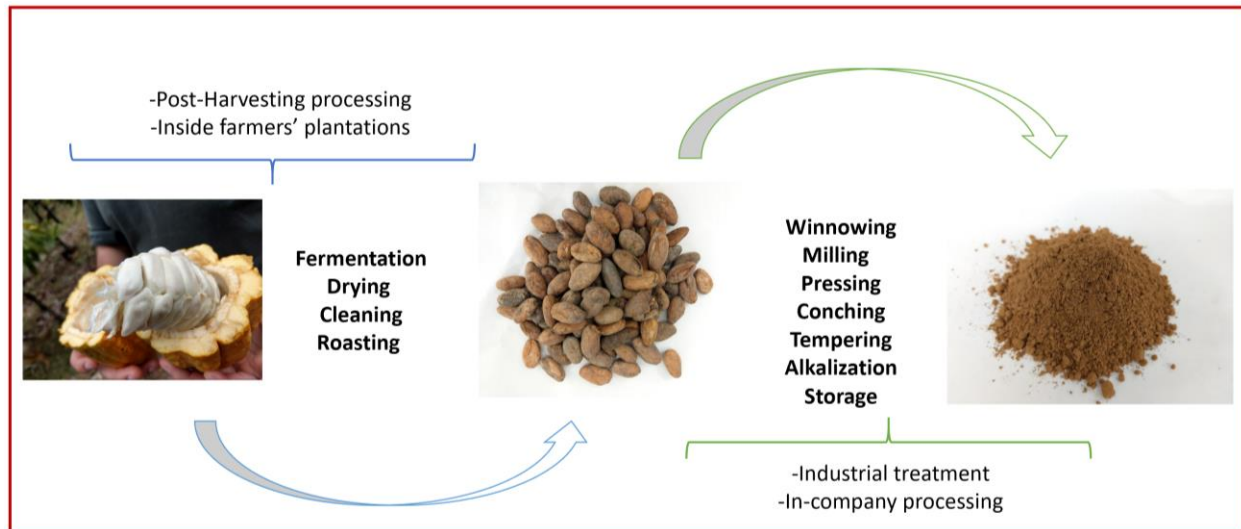
Figure 1.1. Standard process steps from cocoa fruit to cocoa powder.

Cocoa beans are ground to obtain cocoa liquor, which contains two main physical phases: liquid and solid phases. The liquid phase is continuous and composed of triglycerides called cocoa butter, and the solid phase comprises the cocoa particles suspended in this medium (Venter et al., 2007). The pressing step partially removes the cocoa butter and produces an intermediate product called cocoa cake, which then undergoes the milling process to produce cocoa powder (Alshekhli et al., 2011).

The industrial scale-up processing of cocoa possesses several challenges such as the lack of analytical tools to predict the behavior of intermediate products and the economic variables involved in the processes (Alshekhli et al., 2011). For the latter, the circular economy of the residual waste of cocoa shells and cocoa husks has become a promising source for organic material applications (Vásquez et al., 2019). The food industry uses cocoa powder to produce value-added cocoa products, such as chocolate-milk drinks and chocolate bars.

1.2   Description of the Problem

At an industrial scale, cocoa powder presents material handling difficulties through its flowability and stickiness properties. Figure 1.2 shows the cocoa cake after the pressing process. It should be noted that the pressing process determines the content of lipids in the cocoa powder; therefore, the pressure applied during this step varies the lipid content of the cocoa cake.

Figure 1.2. Cocoa cake after the pressing of cocoa liquor.

Thereafter, the cocoa cake was ground to obtain the cocoa powder. Interestingly, the production staff of the chocolate company commented on the powder flow problems; however, they also remarked that not all batches had the same drawbacks. Figures 1.3 and 1.4 illustrate the difficulties occurring during the milling process and transportation through the pipes due to the low flowability of cocoa powder. Figure 1.3 also reveals the material losses during the pipe-cleaning process. Similar issues such as caking behavior and stickiness have been reported in the literature, and they are described in Chapter 2 of this study.

Chapter 2 describes previous studies on powder flowability, particle microstructure, and surface energetics for various complex food and pharmaceutical materials. The lessons learnt from these previous studies have helped us to develop characterization methods for measuring the surface, physical, chemical, and mechanical properties of cocoa powders in this current study.

Some questions regarding the flowability and stickiness of the cocoa powder appear as follows:

1. How does the microstructure of cocoa powders affect their performance-related properties?

2. What are the main differences in terms of surface and bulk properties of cocoa powders that are available in the Colombian market?

Figure 1.3. Milling machine used in the transformation of cocoa cake into cocoa powder.

The flowability of cocoa powder is not yet fully understood, and at the industrial scale, inconveniences are still notorious as the figures display. These industrial issues cause material losses during production and affect the cleaning process in machine handling. Therefore, the influence of the microstructure on the performance of cocoa particles becomes relevant in comprehending its flowability and stability issues.

Figure 1.4. Cocoa powder transported through pipes and the losses in cleaning steps.

1.3 Cacao for Peace Initiative

This work is a part of the "Cacao for Peace (CfP)" initiative to strengthen cocoa production in Colombia. It is recognized that the chocolate manufacturing industry faces challenges in the field of particle technology in cocoa powder handling during production. Thus, there is a need for improvements in the powder behavior such as stickiness, agglomeration, and flow. Although there have been studies that describe the physicochemical bulk properties and chemical composition of cocoa, limited information exists on the surface properties of complex cocoa systems. The aim of this research is to understand the impact of surface characteristics on the physical performance and stability of complex cocoa powder systems. The research presented herein could help this initiative by implementing some of its findings. The materials used in this study are obtained from Colombian companies.

1.4 Project Overview

This research aims to understand the microstructural properties of commercial cocoa powders available in the Colombian market. In this study, three types of cocoa powders obtained from two different companies were chosen as per their availability in the Colombian food market. After a visit to one of the company's production plant, we evaluated the cocoa powders based on their rheological, surface, and bulk properties. This work not only provides the basis for future studies on cocoa powder performance, but also contributes and expands the existing knowledge of cocoa powder investigations for our research group at Purdue University and fills the knowledge gap in the concerned literature.

This dissertation is divided into four chapters. Chapter 2 describes the literature related to cocoa powder and performance-related physical properties. Chapter 3 provides information on the physicochemical and rheological characteristics of the powders considered in this study. Chapter 4 describes the thermal and surface properties and its relationship with water diffusion in the cocoa particles. Chapter 5 presents information on the thermodynamic parameters of the system and the thermal properties of cocoa powders measured by inverse gas chromatography (IGC).

1.5   References

Abbott, Philip. C., Benjamin, Tamara. J., Burniske, Gary .R., Croft, Marcia .M., Fenton, Marieke. C., Kelly, Colleen. R., Lundy, Mark. M., Rodriguez, Fernando., Wilcox, M. (2018). An analysis of the supply chain of cacao in colombia. Technical report.

Alshekhli, O., Foo, D., Hii, C., & Law, C. (2011). Process simulation and debottlenecking for an industrial cocoa manufacturing process. Food and Bioproducts Processing, 89(4), 528-536.

Ascrizzi, R., Flamini, G., Tessieri, C., & Pistelli, L. (2017). From the raw seed to chocolate: Volatile profile of Blanco de Criollo in different phases of the processing chain. Microchemical Journal, 133, 474-479.

Beg, M., Ahmad, S., Jan, K., & Bashir, K. (2017). Status, supply chain and processing of cocoa - A review. Trends in Food Science & Technology, 66, 108-116.

Bruinsma, K., & Taren, D. (1999). Chocolate: Food or Drug? Journal of the American Dietetic Association, 99(10), 1249-1256.

Dand, R. (2011). The physical market in the international cocoa trade. The International Cocoa Trade, 94-118.

García-herrero, L., Menna, F., & Vittuari, M. (2019). Sustainability concerns and practices in the chocolate life cycle : Integrating consumers ' perceptions and experts ' knowledge. Sustainable Production and Consumption, 20, 117-127.

Giacometti, J., Jolić, S., & Josić, D. (2015). Cocoa Processing and Impact on Composition. Processing and Impact on Active Components in Food, 605-612.

Mujica, M., El, A., & Scala, P. (2019). On the logistics of cocoa supply chain in Côte d ' Ivoire : Simulation-based analysis. Computers & Industrial Engineering, 137(September), 106034.

Perego, P., Fabiano, B., Cavicchioli, M., & Del Borghi, M. (2004). Cocoa Quality and Processing: A Study by Solid-phase Microextraction and Gas Chromatography Analysis of Methylpyrazines. Food and Bioproducts Processing, 82(4), 291-297.

Recanati, F., Marveggio, D., & Dotelli, G. (2018). Science of the Total Environment From beans to bar : A life cycle assessment towards sustainable chocolate supply chain. Science of the Total Environment, 613-614, 1013-1023.

Steinberg, F., Bearden, M., & Keen, C. (2003). Cocoa and chocolate flavonoids: Implications for cardiovascular health. Journal of the American Dietetic Association, 103(2), 215-223.

Vásquez, Z., de Carvalho Neto, D., Pereira, G., Vandenberghe, L., de Oliveira, P., Tiburcio, P., . . . Soccol, C. (2019). Biotechnological approaches for cocoa waste management: A review. Waste Management, 90, 72-83.

Venter, M., Schouten, N., Hink, R., Kuipers, N., & de Haan, A. (2007). Expression of cocoa butter from cocoa nibs. Separation and Purification Technology, 55(2), 256-264.

2. BACKGROUND

2.1 Properties of Cocoa powder system

Cocoa powder has been used as a raw material for a wide variety of products in the market, including cocoa beverages, chocolate bars, and chocolate drinks. Cocoa powder has been described as a multi-component system that undergoes changes in the particles due to external stress factors. The physical and chemical properties of the cocoa particles are critical for the performance of the final cocoa powder products. This chapter presents the importance of understanding and manipulating the physical properties of the cocoa complex system in an effort to produce a consistent quality product. The cocoa system is composed of two main parts: solid units (cocoa solids) and the lipid phase (cocoa butter). The cocoa solids are embedded in the lipid phase, which is predominantly located at the surface of the particles. Therefore, this characteristic may explain the degree and extent of lipids affecting the powder performance.

Concerning the manufacturing steps from cocoa nibs to cocoa powder, the quality is a reflection of the specific unit-level operations during processing. The macroscopic characteristics are directly associated with the microscopic particle aspects. Thus, this research aims to assess the surface properties with an emphasis on the lipid phase followed by the response to physical performance and stability.

Cocoa is a cohesive powder, and difficulties are encountered during its handling in the manufacturing processes. Solid-state and physical changes of the particles jeopardize their performance and stability. Moreover, the role of lipid content on the cohesive behavior of cocoa particles needs to be addressed in order to understand the technical issues and manipulate properties for desirable performance (Wojtkowski et al., 2013; Cuq et al., 2011).

2.1.1 Chemical composition

Cocoa-based products contain an extensive number of chemical compounds, and their derivatives are used in food and cosmetics industries. The chemical components are described in this sub-section, and the physical properties are described in section 2.2.2.

The development of flavors in cocoa products depends on the variables involved during fermentation, alkalinization, and roasting processes, which highly influence the promotion of aromatic compounds (Mueller & Kuzmeski, 1994). The aroma of cocoa can be chemically ascribed to pyrazine and the Strecker aldehyde compounds besides around 550 other volatile chemical components that have been identified in cocoa powder. In addition, odorant compounds like acetic acid, 3-methylbutanal, and 2-methylbutanal are present in abundance (Frauendorfer & Schieberle, 2006)

Phenolics and melanoidins are found in cocoa powder, and their proportions depend upon the cocoa variety and roasting process. Interestingly, positive health benefits have been attributed to these compounds (Quiroz-Reyes & Fogliano, 2018). Fermentation reduces the number of total oxalates present in the cocoa beans; however, insoluble oxalates cannot be reduced without enzymatic treatment (Nguyễn et al., 2018), but rather with an alkali solution leading to a higher content of tannic (Mueller & Kuzmeski, 1994). Figure 2.1 displays the relationship between the main quality characteristics of cocoa powder and the respective unit operations.
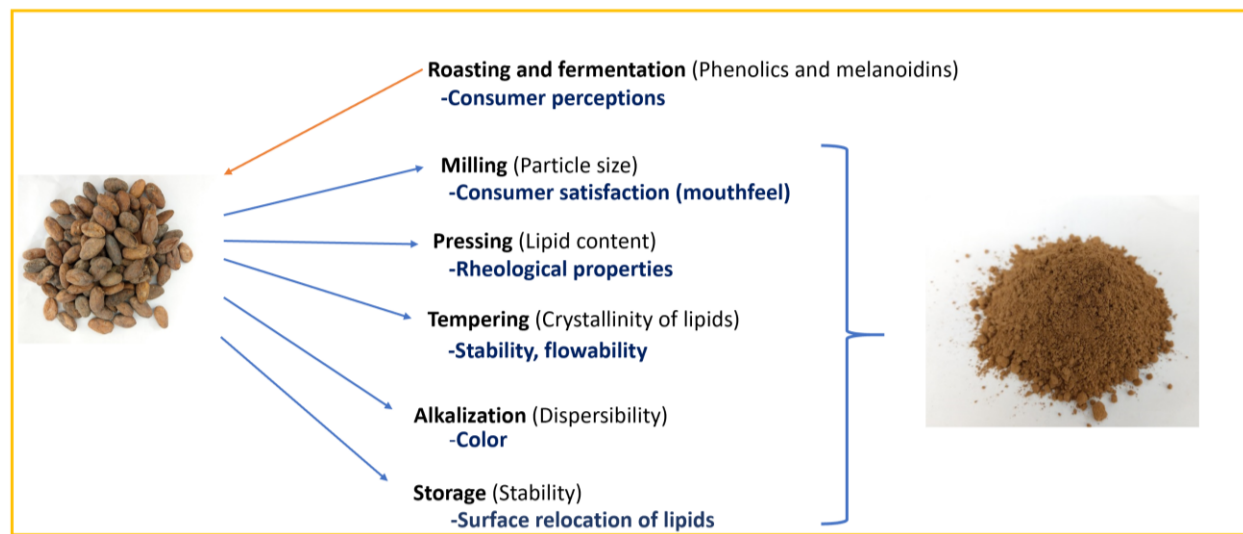
Figure 2.1. Quality attributes of cocoa powder in the respective process steps.

Cocoa fatty acids constitute the main component of cocoa beans. The differences in the solid-states of triacylglycerols influence several physicochemical characteristics such as

crystallinity and melting point, and these differences make cocoa lipids a unique raw material for highly specific applications in cosmetic, food, and pharmaceutical products (Afoakwa, 2014).

The lipids of cocoa beans are stored in the cotyledons. The lipid composition of cocoa beans, cocoa cake, and cocoa powders are summarized in Table 1.2 (Afoakwa, 2014; Reinke et al., 2015; Ghazani & Marangoni, 2018). The packing structure of fatty acids or triacylglycerols is referred to as polymorphism, structures consequential from the number of those compounds within the unit cell is called polytypism (Ghazani & Marangoni, 2018).

Table 2.1. Content and compositional ratios of cocoa lipids.

Cocoa bean dry basis (unfermented)		Cocoa cake and Cocoa powder	
45–60% of lipids (Afoakwa, 2014).		10–12% in low lipid products 22–24% in high lipid products (Afoakwa, 2014).	
95% fatty acids	**5% other components**	**95% triacylglycerols**	**5% other components**
26.5% Palmitic fatty acid 35.4% Stearic fatty acid 34.7% Oleic fatty acid 3.4% Linoleic fatty acid (Afoakwa, 2014)	Monoglycerides and diglycerides Sterols Phospholipids Lauric acid Myristic acid (Afoakwa, 2014)	Variable proportions of the three key triglycerides upon process 1,3-dipalmitoyl-2-oleoylglycerol (POP) 1,3-distearoyl-2-oleoylglycerol (SOS) 1,3-Palmitoyl-stearoyl-2-oleoyl-glycerol (POS) (Reinke et al., 2015; Ghazani & Marangoni, 2018)	2% diacylglycerols <1% monoacylglycerol <1% polar lipids <1% free fatty acids (Afoakwa, 2014)

The chemical structures of POP, SOS, and POS are displayed in Figures 2.2–2.4. The orientation of the triglyceride molecules inside a unit cell influences the thermal and mechanical properties of the system.

1,3-dipalmitoyl-2-oleoyl-glycerol
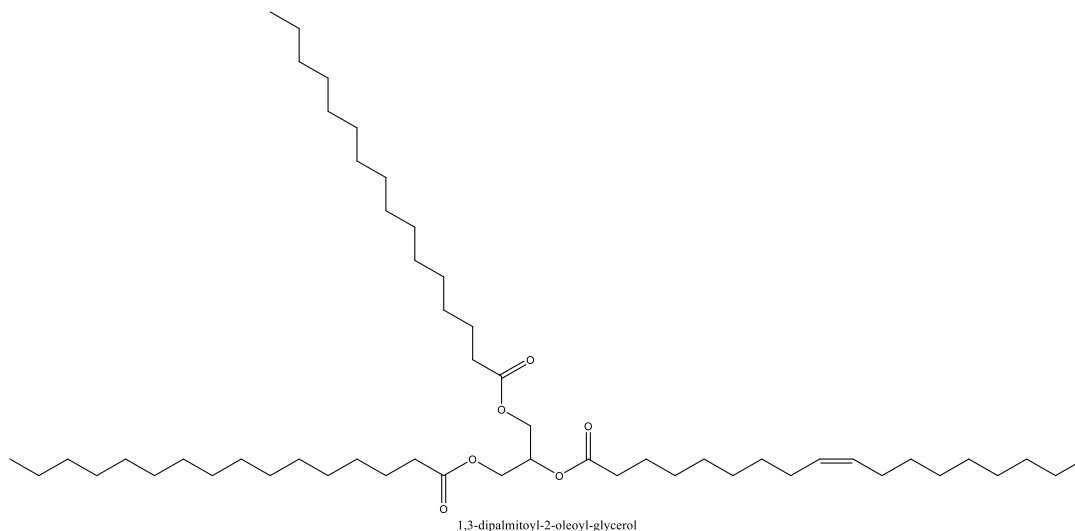
Figure 2.2. Chemical structure of POP.

The lipid phase of the cocoa powder contains all the triglycerides, as mentioned above. Processing conditions such as pressing and milling of the cacao seeds induce organizational changes through tempering of the powders. The crystalline structure of the lipids is influenced by cocoa solid particles (Palmieri & Hartel, 2019), and multiple crystalline structures can be found in the cocoa lipid phase. The number of possible polymorphic forms is still a subject of investigation (Ghazani & Marangoni, 2018).

1,3-Distearoyl-2-oleoylglycerol
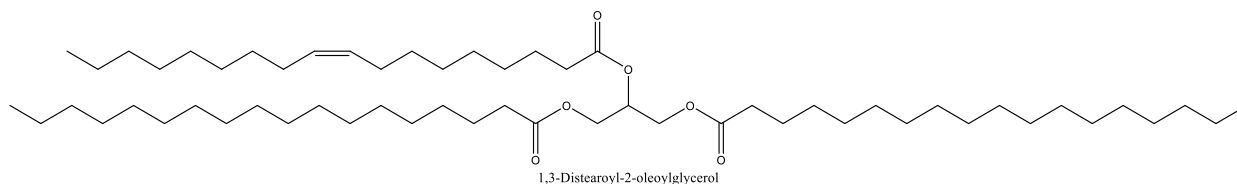
Figure 2.3. Chemical structure of SOS.

Numerous arrangements are present in the cocoa lipid phases of various products. This phenomenon makes the system very challenging for a fundamental understanding when using a

crystallographic approach. Consequently, a description of the lipid polymorphic forms in cocoa powder is commonly missing in the literature.

1,3-Palmitoyl-stearoyl-2-oleoyl Glycerol
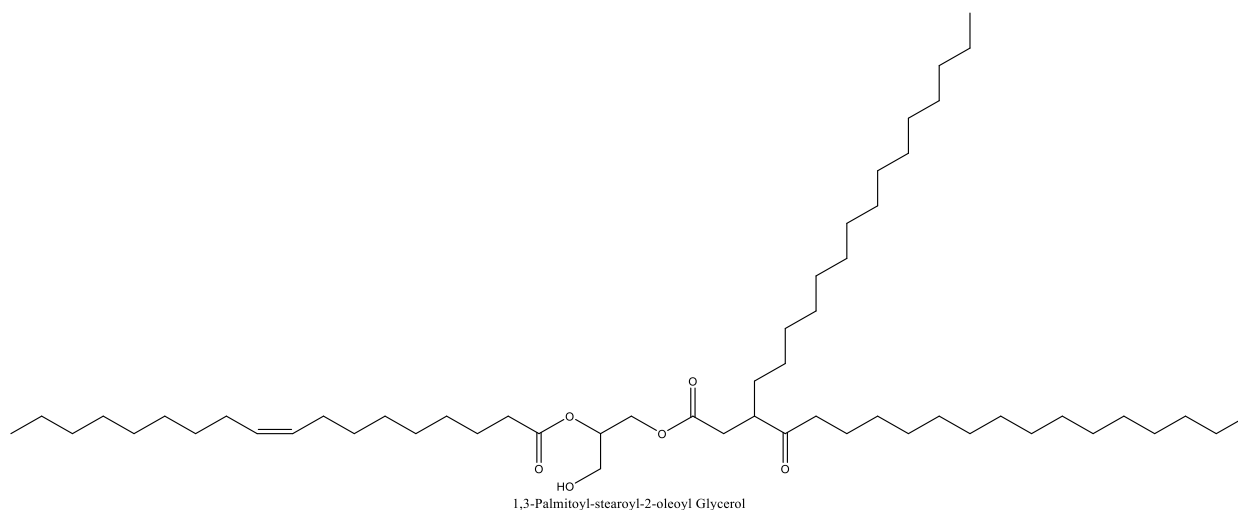
Figure 2.4. Chemical structure of POS.

Cocoa triglycerides have been identified to most commonly exhibit six structural arrangements that can be differentiated by their melting points (Afoakwa, 2014; Reinke et al., 2015; Ghazani & Marangoni, 2018). Table 2.2 describes the ranges of temperatures and nomenclature of the most commonly known polymorphisms of cocoa lipids.

Table 2.2. Melting point and nomenclature of lipids polymorph.

Temperature range of melting point		Crystallographic nomenclature	Numerals nomenclature
(Afoakwa, 2014)	(Reinke et al., 2015)		
16–18 °C	-	γ	I
22–24 °C	-	α	II
24–26 °C	-	β'_2	III
26–28 °C	25.6–27.5 °C	β'_1	IV
32–34 °C	30.8–33.87 °C	β_2	V
34–36 °C	32.3–36.3 °C	β_1	VI

For an enantiotropic system, the stability of the polymorphs increases with the melting point, resulting in denser packing and affecting the compaction and particle density of the cocoa

particles. Thus, depending on the unit cell structure of the polymorphic lipids, exposure of a different arrangement of the functional groups is expected at the surface.

2.1.2 Physical performance

Cocoa powder is routinely used in the confectionery industry. It is the main ingredient with quality perceptions of consumer gratification because of its organoleptic properties, but it is not always present in the highest quantity in chocolate beverages or chocolate products (Benkovic & Bauman, 2011; Quiroz-Reyes & Fogliano, 2018). The importance of physical properties and surface chemistry characterization is appropriate for understanding the behavior of this type of complex powder systems. With that identification and understanding, one can propose the control or manipulation of the surface to improve handling, flowability and stability of the cocoa powders.

Understanding its behavior requires knowledge of its physical properties based on the chemical structure and components (Table 2.1). As indicated in section 2.1.1, cocoa contains a butter phase (POP, SOS, and POS) and a solid phase. The main component of cocoa butter is triglyceride, which is characterized by the esterification of fatty acids with a glycerol chain (Reinke et al., 2015; Ghazani & Marangoni, 2018). The cocoa solids are located at the core where lipids do not accumulate (Jacquot et al., 2016). This phenomenon is relevant for stability upon storage, and it occurs when lipids move from the internal phase in the cocoa solids to the surface level, thus changing the ratio of lipid surface to the core (Jacquot et al., 2016). This phenomenon also influences the handling and flowability of the powder due to particle cohesion-adhesion interactions (Kim et al., 2002; Jacquot et al., 2016). Conversely, particle cohesion and adhesion interactions at the surface have been assessed using surface energetics, demonstrating their influence on the behavior and performance of powder-based food systems (Charmarthy et al., 2009).

The cohesiveness of powders is usually problematic for the powder flow performance. Benkovic et al. (2013a) characterized the cohesive behavior of different conventional food powders, including cocoa with a fat content of 16–18% w/w. It was concluded that the low flowability of the tested food powders was the result of a remarkably high cohesion index of ~19.54 and a small particle size (indicating large surface area). In another study, Wojtkowski et al. (2013) studied two samples of cocoa powder with 12% and 22% lipid contents. In this experiment,

the shear sliding and slumping events in a rotatory drum were evaluated in order to understand the dynamic performance of the cohesive powder. Although the cocoa powder containing 12% lipids had smaller particles, it showed better flowability due to the occurrence of more shear sliding events than that in the cocoa powder containing 22% lipids.

Comparing the cohesion properties of the two pure cocoa systems with 10–12% and 16–18% lipid content, Benkovic et al. (2013b) quantified the compaction and cohesion index by measuring the maximum compression and decompression forces when a rotating blade was moved downward and upwards, respectively. The results of the cocoa powder with 10–12% lipid content showed smaller particle size, higher compression force, and lower decompression force compared to those of the counterpart material containing 16–18% lipid content. In addition, the cocoa powder containing higher fat content exhibited a lower mean cake strength (Benković et al., 2013b). Furthermore, Petit et al. (2017) demonstrated that the caking strength was weaker for the cocoa sample with 21% lipid content than that with 11% lipid content.

The appreciation of the findings described in the above paragraph raised the motivation towards investigating the extent to which the particle size and fat content are correlated with the performance behavior of cocoa samples, and the properties that will predominantly influence the cohesive interactions, caking, flowability, and wettability of these particular cocoa powders.

The cohesive interactions are predominantly manifested in particle sizes below 200 µm. The cocoa powder is very cohesive in nature as the particle size ranges from 20–40 µm. In an attempt to break the strength of the cohesive forces, several approaches including agglomeration and mixing unit operations have been carried out. Agglomeration of cocoa using steam increased the particle size up to 212–850 µm (Vissotto et al., 2014). In the mixing process of particles in a rotatory drum, fine cohesive particles cohered with each other to form large particles of sizes ranging from 850 µm–1250 µm and improved the homogeneity of the products (Jarray et al., 2019). It was reported in a study on a cocoa beverage product that large-sized particles affect wettability; thus, an increase in the fraction of fine particles has been attributed to an increase in wetting times (Hla & Hogekamp, 1999).

Cohesive interactions also play a role in the caking phenomenon. The caking behavior of cocoa has been attributed to the solid-state properties of the cocoa butter. Palmieri and Hartel (2019) studied the crystallization of cocoa butter during the pressing process with controlled tempering conditions, and they evaluated the effects of the alkalization step and total fat content on the caking

behavior of the cocoa powder matrix. The study used both low-fat (8–12%) and high-fat (20–24%) cocoa powders and evaluated the results by a qualitative inspection on the amounts of powder that adhered to metal balls after tumbling. It was found that the physical state of the cocoa lipids modified the caking behavior rather than the lipid content. The high-lipid content cocoa was treated with a pre-crystallization step and displayed a comparable caking tendency to those displayed by the low-lipid content samples. In addition, the pre-crystallization process of the cocoa solids embedded in the powder matrix was conferred to the most thermodynamically stable lipid polymorph (Palmieri & Hartel, 2019).

The water content of cocoa powders controls the flowability properties. The powder flow was measured with a shear cell to determine the decrease in flow index caused by the increase of water content in the cocoa samples (Ostrowska-Ligeza & Lenart, 2015a). This decrease in flow index was attributed to the increase in cohesion forces due to the presence of water, even though the surface of cocoa particles is lipophilic (Ostrowska-Ligeza & Lenart, 2015b). Although water does not affect the plasticization behavior of cocoa, the caking strength increases at a high temperature and humidity (Chavez et al., 2011). The cocoa cake must be ground to pass through a 200 mesh to obtain cocoa powder that fulfills quality parameters. Agglomeration may occur at this stage because surface interactions become predominant at such particle sizes (Firmanto et al., 2015a). Issues with melting of lipids upon milling were also noticed, particularly in the cocoa cake containing 26.8% fat. To prevent the occurrence of this issue and to increase the process efficiency, the optimal temperature should be in the range of 25–26 °C (Firmanto et al., 2015b). However, the glass transition temperature (Tg) of cocoa powder is not detected by differential scanning calorimetric (DSC) analysis (Chavez et al., 2011).

The cohesion properties of cocoa powders with a lipid content of 12% have been determined by addressing the unconfined yield stress of the powder under specific consolidation stresses using a lambdameter and a FT4 powder rheometer (Imole et al. 2016). Bulk cohesion was calculated by yield loci analysis at the lowest normal consolidation and found to be 7.4 kPa. It was concluded that a five-fold increase in the normal consolidation increases the bulk cohesion to 41.8 kPa, thus, the bulk properties of these systems cannot differentiate this performance (Imole et al., 2016).

The importance of surface energetics and chemical characterization to understand the behavior of food powders such as lactose (Charmarthy et al., 2009), starch (Martinez et al., 2018),

rigid silica bead particles coated with lipids (Jange & Ambrose, 2019), and cocoa and coffee powders (Chavez-Montes et al., 2019) on flowability performance has been widely accepted.

Based on the above discussion, it can be said that several attributes of cocoa play an important role toward powder behavior; however, the need of understanding the extent and degree to which the various parameters contribute to the performance and stability of the cocoa systems still persists. Thus, the agglomeration, caking, flowability, and wettability of cocoa powder need to be evaluated based on approaches of surface chemistry (surface-lipid approach), energetics characterization, and solid-state and particle morphology. Therefore, these aspects of cocoa will be the focus of the following chapters.

2.1.3 Functionality in products

This sub-section presents the role of pure cocoa powders in the performance of cocoa beverages. Additives are included in cocoa products to enhance the physical and chemical characteristics and increase the consumer acceptability of the final products. In this context, lecithin (emulsification and lubricant properties) is frequently added to improve the dispersibility of cocoa beverages. Typically, after processing the cocoa powder with sugars, a lipid phase covers the clusters forming a sugar–cocoa assembly. The addition of lecithin during the conching process increases the hydrophilicity of cocoa beverage particles (Dimick & Hoskin, 1981).

Benkovic et al. (2011) used fluidized-bed agglomeration to prepare different cocoa beverages and evaluated the bulk density, Hausner ratio, and physical properties of the agglomerates. Cocoa powder agglomerates with 16–18% lipid content was not less denser than the mixtures of the raw materials. Two agglomerate products of cocoa powder with 10–12% of lipids showed higher bulk densities than the non-agglomerated ones. Powder flowability determined by the Hausner ratio classification did not distinguish between the cocoa beverages prepared with 10–12% and 16–18% lipid content. Sugar is another additive added to the cocoa beverage to influence wetting, dispersibility, and dissolution properties (Abdelaziz et al., 2014). Typical sugar additives for this type of products are lactose and sucrose; they are used at various compositional ratios. A simple dry mixing process was used to prepare the cocoa–sugar systems. By measuring the change in particle size (D_{50}) over a time of 900 s for the reconstituted product (Abdelaziz et al., 2014), it was recognized that lactose–cocoa mixtures have significantly low wetting times. In addition,

lactose–cocoa mixtures enhance dispersibility, whereas sucrose–cocoa mixtures increase solubility.

The crystallization of the cocoa butter is also affected by the addition of sugar and lecithin. As mentioned in section 2.2.1, the cocoa lipids exhibited improvement in their crystallization to a higher energetic polymorph when cocoa solids were present. Similar results have been reported for chocolate systems, where the formation of heterogeneous nucleation for triglycerides with a low degree of crystallinity is observed by sugar addition (Svanberg et al., 2011). The two main requirements, that seem to dominate the crystallization of lipids in the presence of cocoa solids, are as follows: a) hydrophilicity offers higher affinity for crystal–seed nucleation, and b) a lower particle size increases crystallization to higher energetic lipid polymorphs (Svanberg et al., 2011). An increase in the hardness of cocoa confectionery products is explained by the polymorphic states of the lipids. Kalic et al. (2018) found that a higher content of saccharides in the cocoa matrix increases the nucleation of less denser polymorphs. Conversely, the presence of cocoa solids increased the growth of denser polymorphs (Kalic et al., 2018), which is in line with the postulation of Svanberg et al. (2011).

Sedimentation of cocoa solids is a common issue when consumers prepare instant chocolate drinks. When sedimentation occurs, an increase in dispersibility and wettability of the powder is necessary. Various attempts to improve the physical properties of cocoa-based beverages by different processes have been made, such as spray drying (Selamat et al., 1998), fluidization (Benkovic et al., 2011), and mixing of additives (Guneser et al., 2019). For the spray-dried powder, the contributions of alkalizate and lecithin were evaluated. The bulk density of cocoa powders with 10–12% lipid contents was reported to be lower for the spray-dried powder than the unprocessed materials. It was reported that the dispersibility decreased for the alkalized powder with a particle size that passed through a 0.43 mesh sieve, while the soy lecithin content did not affect the dispersibility at all (Selamat et al., 1998). An approach to prevent sedimentation is the addition of additives (mainly sugar), and it should be added after the pasteurization process in a pre-heated milk solution (Guneser et al., 2019).

The inclusion of sucrose in instant cocoa malt beverages improved the wettability of cocoa (Wee et al., 2020). A blade grinder was used in the cocoa paste agglomerate before the addition of sucrose. An increase in the sucrose content resulted in a decrease in particle size and consequently, improved the wetting time (Wee et al., 2020). Shittu & Lawal (2005) found that fat content in the

range of 2–11% and particle size did not correlate with the wettability properties of the cocoa beverage. Nevertheless, dispersibility and wettability in instant products were remarkably improved by the addition of sucrose (Wee et al., 2020).

2.2 Motivation

The role of lipid-content, additives and processes in for different applications of cocoa beverage products was emphasized in the previous section. Interestingly, most of the existing studies have failed to explain the differences encountered when dealing with cocoa powders processed differently and in those containing different lipid contents and additives that contribute to the agglomeration, caking, wettability, dispersibility, and dissolution of the cocoa-based systems. Clearly, there is a need for a better understanding of the overall characteristics and performance of cocoa, as a material and as a product. The research presented herein aims to contribute to this knowledge.

2.3 References

Abdelaziz, I., Sahli, A., Bornaz, S., Scher, J., & Gaiani, C. (2014). Dynamic method to characterize rehydration of powdered cocoa beverage : In fl uence of sugar nature, quantity and size. Powder Technology, 264, 184-189.

Afoakwa, E.O. (2014). Cocoa processing technology. CRC Press: Taylor & Francis Group, pp. 179-180.

Benkovi, M., & Igor, Š. (2013). Flow Properties of Commonly Used Food Powders and Their Mixtures. Food Bioprocess Technol, 6, 2525–2537.

Benkovi, M., Bel, A., & Bauman, I. (2013). Physical Properties of Non-Agglomerated Cocoa Drink Powder Mixtures Containing Various Types of Sugar and Sweetener. Food Bioprocess Technol, 6, 1044–1058.

Benkovi, M., & Bauman, I. (2011). Agglomeration of cocoa powder mixtures : Influence of process conditions on physical properties of the agglomerates. Journal on Processing and Energy in Agriculture, 15, 46-49.

Chamarthy, S., Pinal, R., & Carvajal, T. (2009). Elucidating Raw Material Variability - Importance of Surface Properties and Functionality in Pharmaceutical Powders. AAPS PharmSciTech, 10, 780-788.

Chavez-Montes, E., Martínez-alejo, J., Lozano-perez, H., Gumy, J., Zemlyanov, D., & Carvajal, M. (2019). A surface characterization platform approach to study Flowability of food powders. Powder techonology, *357*, 269-280.

Chavez M, E., Santamar, A., Gumy, J.C., Marchal, P (2011). Moisture-induced caking of beverage powders. J Sci Food Agric, 91. 2582-2586.

Cuq, B., Rondet, E., & Abecassis, J. (2011). Food powders engineering, between knowhow and science: Constraints, stakes and opportunities. Powder Technology, 208, 244-251.

Engeseth, N.& Pangan, M. (2018). Current context on chocolate flavor development — a review. Current Opinion in Food Science, *21*, 84-91.

Firmanto, H., & Suharyanto, E. (2015). Performance of Cooled Cone Grinding Machine. , 31(2), 119-129.

Frauendorfer,F & Chieberle, P. (2006). Identification of the Key Aroma Compounds in Cocoa Powder Based on Molecular Sensory Correlations. J. Agric. Food Chem, 54, 5521-5529.

Ghazani, S & Marangoni, A.G. (2018). New Insights into the β Polymorphism of 1,3-Palmitoyl-stearoyl-2- oleoyl Glycerol. Crystal Growth & Design, 2018 *18* (9), 4811-4814

Hla, P., & Hogekamp, S. (1999). Wetting behaviour of instantized cocoa beverage. International Journal of Food Science and Technology, 335-342.

Imole, O., Paulick, M., Magnanimo, V., Morgeneyer, M., Chávez Montes, B., Ramaioli, M., . . . Luding, S. (2016). Slow stress relaxation behavior of cohesive powders. *Powder Technology, 293*, 82-93.

Jacquot, C., Petit, J., Michaux, F., Montes, E., Dupas, J., Girard, V., . . . Gaiani, C. (2016). Cocoa powder surface composition during aging : A focus on fat. *Powder Technology, 292*, 195-202.

Jange, C., & Ambrose, R. (2019). Effect of surface compositional difference on powder flow properties. *Powder Technology, 344*, 363-372.

Jarray, A., Shi, H., Scheper, B., Habibi, M., & Luding, S. (2019). Cohesion-driven mixing and segregation of dry granular media. Scientific Reports natureresearch, 9(1), 1-12.

Kalic, M., Krstonosic, V., Hadnadev, M., Beyer, S., Natasa, G., Ljeskovic, J., & Wiking, L. (2018). Impact of different sugar and cocoa powder particle sizes on crystallization of fat used for the production of confectionery products * Particle size distribution influences fat crystallization. J Food Process Preserv, 42, 1-9.

Kim, E., Chen, X., & Pearce, D. (2002). Surface characterization of four industrial spray-dried dairy powders in relation to chemical composition , structure and wetting property. Colloids and Surfaces B: Biointerface, *26*, 197-212.

Landillon, V., Cassan, D., Morel, M., Cuq, B. (2008). Flowability, cohesive, and granulation properties of wheat powders. Journal of Food Engineering, 86, 178-193.

Martinez-Alejo, J.M., Benavent-Gil, Y., Rosell, C.M., Carvajal, T., Martinez, M.M. (2018). Quantifying the surface properties of enzymatically-made porous starches by using a surface energy analyzer. Carbohydrate Polymers 200 (2018) 543-551.

Mueller, W., & Kuzmeski, J. (1944, 11 1). The Determination of Tannic Substances in Commercial Cocoa Powders. *Journal of Dairy Science, 27*(11), 897-901.

Nguyễn, H., Lê, H., & Savage, G. (2018, 4 1). Effects of maturity at harvesting and primary processing of cocoa beans on oxalate contents of cocoa powder. *Journal of Food Composition and Analysis, 67*, 86-90.

Ostrowska, E.L., Lenart, A. (2015). Influence of water activity on the compressibility and mechanical properties of cocoa products. LWT-Food Science and Technology, *60*, 1054-1060

Palmieri, P., & Hartel, R. (2019). Crystallization of Cocoa Butter in Cocoa Powder. J Am Oil Chem Soc, 96, 911-926.

Petit, J., Michaux, F., Jacquot, C., Chavez, E., Dupas, J., Girard, V., Gianfrancesco, A., Scher, J., Gaiani, C. (2017). Storage-induced caking of cocoa powder. Journal of Food Engineering, *199*, 42-53.

Quiroz-Reyes, C., & Fogliano, V. (2018, 6 1). Design cocoa processing towards healthy cocoa products: The role of phenolics and melanoidins. *Journal of Functional Foods, 45*, 480-490.

Reinke, S., Roth, S., Santoro, G., Heinrich, S., & Palzer, S. (2015). Tracking Structural Changes in Lipid-based Multicomponent Food Materials due to Oil Migration by Microfocus Small-Angle X - ray Scattering. ACS Appl. Mater. Interfaces, 9929-9936.

Roos Yrjö H, & Drusch Stephan. (2016). Food Components and Polymers. In *Phase Transitions in Foods* (2nd ed., chapter 5). Elsevier.

Sanchez-Reinoso, Z., Osorio, C., & Herrera, A. (2017, 8 1). Effect of microencapsulation by spray drying on cocoa aroma compounds and physicochemical characterisation of microencapsulates. *Powder Technology, 318*, 110-119.

Selamat, J., Hussin, N., Zain, A., & Man, Y. (1998). Effects of alkalized cocoa powder and soy lecithin on physical characteristics of chocolate beverage powders. Journal of Food Processing and Preservation, *22*, 241-254.

Shittu, T., & Lawal, M. (2007, 1 1). Factors affecting instant properties of powdered cocoa beverages. *Food Chemistry, 100*(1), 91-98.

Svanberg, L., Ahrné, L., Lorén, N., & Windhab, E. (2011, 5 1). Effect of sugar, cocoa particles and lecithin on cocoa butter crystallisation in seeded and non-seeded chocolate model systems. *Journal of Food Engineering, 104*(1), 70-80.

Vissotto, F., Giarola, R., Jorge, L., Makita, G., Maria, G., Quirino, B., . . . Menegalli, F. (2014). Morphological characterization with image analysis of cocoa beverage powder agglomerated with steam. Food Sci. Technol, Campinas, 34(4), 649-656.

Vu, T., Galet, L., Fages, J., & Oulahna, D. (2003). Improving the dispersion kinetics of a cocoa powder by size enlargement. Powder Technology, *130*, 400-406.

Wee, Y. J., Xin, R., Seow, Yi-Xin., Viton, F., & Zhou, W. (2020). Influence of sucrose reduction on powder and reconstitution properties of powdered cocoa malted beverage. *Powder Technology, 360*, 221-230.

Wojtkowski, M., Imole, O., Ramaioli, M., Chavez, M, E., & Luding, S. (2013). Behavior of cohesive powder in rotating drums. Powders and Grains AIP Conf. Proc, 1542, *983*.

3. FLOWABILITY PERFORMANCE OF COCOA POWDERS SYSTEMS

3.1 Abstract

The flowability of food systems has been an ongoing issue in the handling and processing of dry powders. Cocoa particles contain multiple chemical components that are heterogeneously distributed at the core and particle surface. This study focused on the lipids located at the surface and on the physical properties to explain powder flow performance. The flow behaviors of pure commercial cocoa powders, with similar particle size distribution and different fat contents, were tested under dynamic and static conditions using aeration and permeability methods. The obtained results revealed that the flow under aeration conditions was not only caused by the lipid content at the surface but also by the bulk density and surface area properties. This chapter outlines the importance of surface chemistry probing for gaining fundamental insights with regard to powder flow behavior, and ultimately for improving the behavior by controlling the surface lipid heterogeneity.

3.2 Introduction

Cocoa powder is a very cohesive powder with poor flow (Juliano et al., 2006). The flow properties of cocoa powders have been investigated using shear cells to obtain the flow functions by yield loci analysis. However, in industrial handling, fluidized conveyance is required to transport the powder from the milling machine to the storage location. Grinding is a necessary unit operation in cocoa processing, and the resulting particle properties, size, morphology, roughness, and surface interactions (cohesion and adhesion) may affect the fluidization behavior of cocoa powder (Tan & Balasubramanian, 2017; Abrahamsen & Geldart, 1980a; Xie, 1997; Leturia et al., 2014). In a fluidized fine powder setting, particle interactions and gravitational forces are exposed to greater risk, while the frictional forces seem to have a minimal effect on the powder behavior (Baerns, 1966). This study used powder flow characterization methods, under fluidization or dispersion in air, to assess the aeration and compressibility conditions to investigate the behavior of the cocoa powder.

In aeration testing, the expansion of the powder bed is achieved by the air crossing the sample vessel, affecting the bulk properties of the materials, average solid phase packed density, and particle interactions (Abrahamsen & Geldart, 1980b). The speed rate of air passes through the powder bed sample in the vessel and it affects the powder density, fluidization behavior, and particle interactions (Leturia et al., 2014).

In compression testing, the decrease of bulk density is achieved by applying a normal perpendicular stress to the powder in the vessel. The percentage of volume change after compression is calculated to obtain the compressibility index, which serves as an indicator for classifying the cohesive and non-cohesive powder tendencies. A high compressibility index indicates cohesion (Leturia et al., 2014). During the consolidation of cocoa, low angle of internal is observed, and can be explained in terms of the low surface roughness owing to the presence of fat at the surface (Juliano et al., 2006).

There are various instruments that can characterize the powder flow. All techniques incorporate assumptions and have particular advantages and disadvantages. Currently, the FT4 powder rheometer is the preferred method, because it is a reliable device for differentiating the cohesive behavior performance under compression and fluidization in several powder applications (Leturia et al., 2014).

Cocoa particles have an average fine particle size (20–40 µm), which increases by steam agglomeration up to 212–850 µm (Vissotto et al., 2014). The cohesion forces amongst the materials are predetermined based on the range of particle size distribution. In rotatory drum testing, the results obtained by an experiment with 0.85- and 125-mm surface-treated silica particles revealed that, once the cohesion forces increase, the separation amongst the particles decreases and the mixing process is improved (Jarray et al., 2019). Apart from the physical particle properties, in a cocoa beverage system with a particle size d_{50} of 180 µm, the excessive amount of fine particles with a size of $\pm$ 20 µm decreases the instant properties (Wettability, dispersibility, solubility) (Hla & Hogekamp, 1999).

Cocoa exhibits plastic deformation when the powder is subjected to low or high consolidation stresses, which is attributed to the lipid content (Juliano et al., 2006). In the production of cocoa-milk beverages, milk powder is typically ground in combination with cocoa powders. The particle interactions in the plastic regimen are achieved by controlling the grinding temperature above the milk powder's glass transition temperature (Ziegler & Langiotti, 2002).

Inevitably, the components of both milk and cocoa are subjected to stress. Particularly, the lipid components and triglyceride networks depend on the microstructure of the cocoa solid and process parameters (Lechter, 2012). The proportion of cocoa butter in the powder provides advantages to the rheological properties of chocolate products and intermediates (Fang et al., 1994). This study investigated the role of the total and surface lipid content on the cohesive behavior of particles and the viscoelastic characteristics of cocoa through aeration and permeability testing using the FT4 rheometer (Freeman Technology, UK).

3.3   Materials and methods

3.3.1   Materials

Three cocoa powders with different fat content, namely, Material 1 (M1), Material 2 (M2), and Material 3 (M3), were used as received for the experiments, unless otherwise indicated. The M1 and M2 batches were obtained from company A manufactured under the same process, but with different total fat content. The M3 batch was obtained from company B processed and manufactured under conditions different to those of batches M1 and M2.

3.3.2   Aeration test

Aeration testing was carried out using an FT4 rheometer, because it is a suitable technique for differentiating the cohesiveness of various cocoa powders. Briefly, air is introduced into the base of the vessel to fluidize the powder. Once the powder is exposed to the air flow, the flow rate gradually increases. Before performing the aeration test, the powder undergoes several conditioning cycles. A homogeneous powder sample is achieved by removing the previous stress forces. The energy required for the blade to move through the powder is related to the force and torque required to move the powder inside the vessel.

The basic flow energy is measured with the rotational blade at different air velocities to assess the powder fluidization. Approximately 40–50 g of the powder were weighted and placed in the experimental vessel. The air velocity of 0, 2, 4, 6, 8, and 10 mm/s was configured for test analysis, and measurements were made in triplicate.

3.3.3 Permeability test

This method involved a Venten piston, which applied a continuously preset normal load. Additionally, using an automated procedure, the air flow passed from the bottom part of the powder bed and the powders were filled up to the upper part of the vessel under standard operating conditions. The air pressure difference through the lowest side and higher side of the vessel was measured. The normal stresses of 0, 2, 4, 6, 8, 10, 12, and 14 kPa were applied during the test. The powder permeability is inversely proportional to the pressure drop, which changes the powder bed and compressibility of the materials. Measurements were made in triplicate using the FT4 rheometer.

3.3.4 Particle size analysis

The particle size was measured by laser scattering in a Malvern MasterSizer 3000 apparatus (Malvern Instruments Ltd, United Kingdom). Approximately 30 mL of the powders were placed in the dry dispersion unit, and 45% of the feed tray's maximum speed was used to control the flow of the material to reach an obscuration between 2 and 10%.

3.3.5 Particle true density

True density measurements were carried out in in an Accupyc II 1340 Pycnometer Helium gas (Micromeritics, GA, U.S.A.) according to the ASTM B923-16 standard. The instrument was calibrated before use. A Metter-Toledo XS105 Dual-Range analytical balance was used to measure the mass of the samples contained in a 3.5-cm^3 chamber, and ten consecutive cycles were performed per sample.

3.3.6 Surface lipid extraction

The powder surface fat phase extraction procedure was adopted from Jacquot et al. (2016) and Petit et al. (2017). A sample with approximately 10 g of cocoa powder was placed in an Erlenmeyer flask. Then, 50 mL of Petroleum Ether ACS (Fisher Scientific, NJ, USA) were added and stirred at a speed of 200 rpm for over 1 min. The fat extracted from the particles was collected in a Büchner funnel with a Whatmann grade 2 filter. The filtered liquid was placed in a round-bottom boiling flask, which was then placed in a Rotavapor® RII (Buchi, Switzerland). The

petroleum ether was evaporated at 40 °C at the rotation speed of 60 rpm. The fat collected in the round-bottom boiling flask was weighed and the free fat percentage at the powder surface was obtained.

3.3.7 Surface area

Inverse gas chromatography (IGC; Surface Measurement Systems, United Kingdom) was used to determine the surface area of the cocoa particles. A salinized column with a 4-mm internal diameter was used, and approximately 450–500 mg of powder were filled into the column; a temperature of 298.15 K and a flow rate of 5 cm^3/min were used. Ethanol was successfully used as a hydrophilic probe molecule.

The use of octane, heptane, or cyclohexane as a probe molecule to calculate the surface area by IGC has been reported (Legras et al., 2015). However, these probe molecules were not suitable for the analysis of the cocoa powder surface area owing to their higher affinity for lipophilicity, which made the retention time higher than 30 min at a flow rate of 5 cm^3/min. Thus, physisorption was not achieved and chemisorption started to occur. A hydrophilic gas probe such as ethanol is suitable because it provides only physisorption interaction between the cocoa particles and the gas probe molecule. To date, the use of ethanol for calculating the surface area using IGC has not been reported.

A method for measuring the surface area was developed using the physisorption of ethanol. Generally, food powders have a small surface area. The International Union of Pure and Applied Chemistry (IUPAC) recommends that surfaces of less than 5 m^{2}g^{-1} use probe molecules with higher atomic mass, such as Krypton and Xenon molecules, in BET standard equipment (Sign et al., 1985). By using IGC, it has been possible to obtain the plausible surface area values. Moreover, interpreting the sorption of probe molecules using IGC is a promising technique for characterizing the surface properties of organic materials (Duralliu et al., 2019).

3.3.8 Particle shape and qualitatively roughness.

Scanning Electron Microscopy (SEM) was used to visualize the particle morphology (shape and surface qualitatively roughness). The samples were coated in a Cressington 208HR sputter device with platinum under an Argon atmosphere for 60 s. The FEI Nova Nano SEM 200

field emission scanning electron microscope (Hillsboro, Oregon, USA) at the Purdue Life Science Microscopy Facility was used, and the electron beam was set to 5.00 kV at a working distance of 5.0 mm.

3.3.9 Thermal analysis

The thermal properties were measured using the Differential Scanning Calorimeter Q 2000 (TA Instruments, New Castle, DE. USA) coupled with a refrigeration system. Hermetically sealed aluminum pans were used to analyze 13-15 mg of the samples. The samples were first cooled to -10.00 °C in an isothermal step for 10 min and subsequently heated to 45.00 °C with an increment of 2.00 °C/min. The analyses were carried out in duplicate: one sample without a cooling step, and another sample with a cooling step.

3.3.10 Statistical analysis

One-way ANOVA was used for statistical analysis, and $p<0.05$ was considered to be statistically significant. OriginPro version 2019b (OriginLab Corporation, Northampton, MA, USA.) was used to produce the graphs and carry out the statistical analysis.

3.4 Results and Discussion

3.4.1 Physical properties

Monomodal particle size distribution was observed in all samples (Figure 3.1). The average particle size, d_{v50}, was in the range 14–17 μm with no significant difference ($p>0.05$) was observed amongst the samples. As has been previously reported, a cocoa product should have a particle size of less than 50 μm to satisfy the quality requirements (Tan & Balasubramanian, 2017).
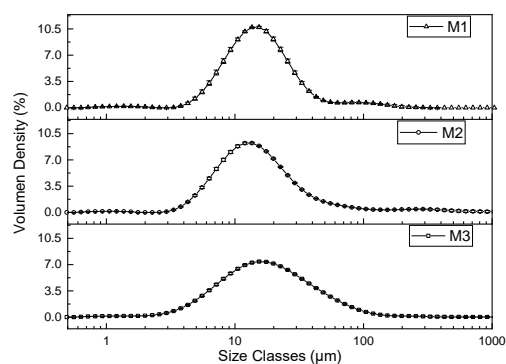
Figure 3.1. Particle size distribution of cocoa particles.

The SEM images for the cocoa particles exhibit agglomeration and a notorious rough surface (Figure 3.2). The cluster particles result from cohesive interactions in the particle size range of 14-17 μm. Additionally, the surface exhibits various molten-looking particles, likely lipids at the surface that contribute to the cohesive forces.
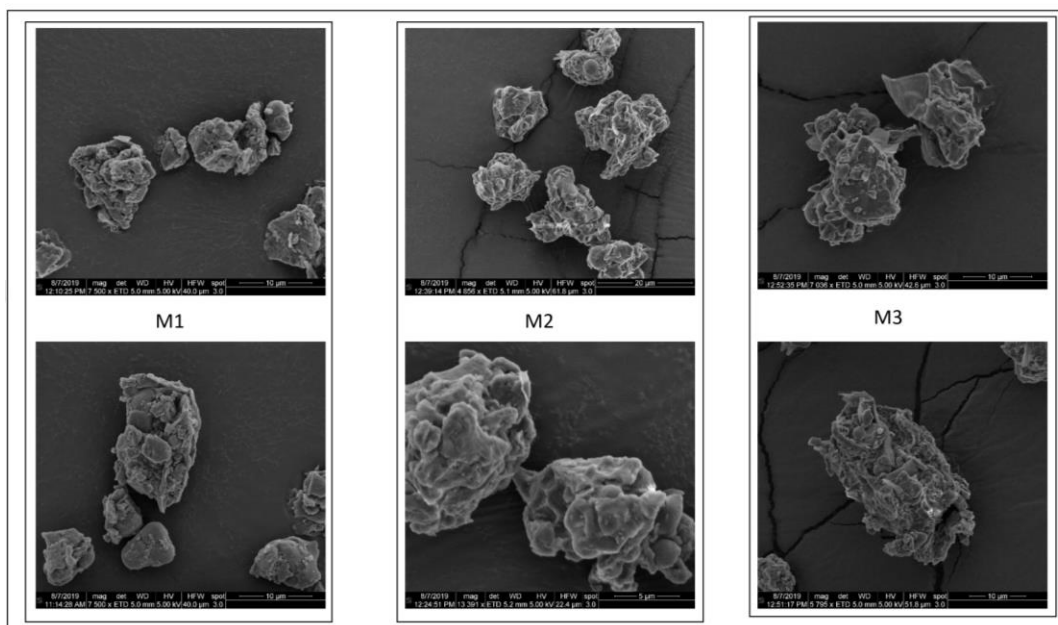
Figure 3.2. Scanning electron microscopy images of cocoa particles.

The average true density for cocoa powders M1, M2, and M3 was 1.2249, 0.9022, and 1.1377 g/cm^3, respectively (Figure 3.3). The true density was significantly different (p<0.05).
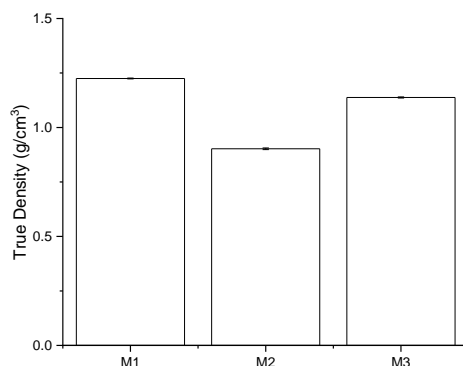
Figure 3.3. True density of cocoa samples.

The lipid content results are presented in Table 3.1. As can be seen, the M2 cocoa powder with low density had lower lipid content compared with M1 and M3.

Table 3.1. Lipid percentage at the surface.

	M1	M2	M3
% Surface lipid content ± S.D.	11.57 ± 1.44	7.51 ± 1.09	19.43 ± 4.45

In the bicomponent system of cocoa powder, the particle density depends on the cocoa lipids and cocoa solids ratio. Moreover, the crystalline structure of the lipids affects the particle density, and the type of polymorphism in the lipids influences the density of the structure (Afoakwa, 2014).

The DSC (Differential Scanning Calorimetry) thermogram exhibited differences in the onset melting point and enthalpy amongst the samples. The M2 cocoa sample with the lowest lipid content at the surface and lowest density exhibited low values for both the onset and enthalpy

(Table 3.2). The other two samples, M1 and M3, exhibited similar enthalpy values. The data obtained seems to indicate that there exists a direct relationship between the lipid content and the enthalpy change. Two polymorphs have been reported for each of the three cocoa samples: for M1, α and β'_1; for M2, α and β'_2; for M3, β'_1 and β_2; and that the cacao lipids with high energetic polymorphs exhibit high packing structure, indicating high density (Afoakwa, 2014). In this study, the low true density of the M2 sample may be explained by the low lipid-packing and onset temperature (Table 3.2).

Table 3.2. Onset of melting point measured by DSC.

	First Onset (°C)	Second Onset (°C)	Enthalpy normalized (kJ/g)
M1	22.67	26.17	16.307
M2	21.47	25.36	11.979
M3	26.96	30.97	16.860

Triglyceride packing is affected by unsaturated lipids, and low packing is linked to a low melting point (Lechter, 2012). The melting events obtained by the DSC provide a qualitative estimation of polymorphic presence in the sample. Moreover, the polymorphism in the cocoa powder influences the cohesive forces amongst the particles. The quantification and polymorph type have to be evaluated using other techniques, such as X-Ray diffraction analysis.

3.4.2 Surface area analysis
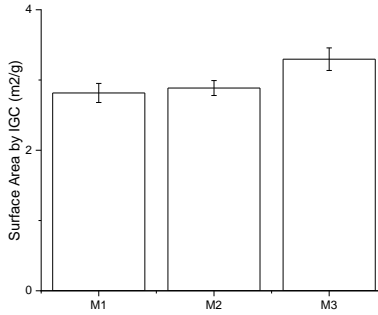
Figure 3.4. IGC Surface area of cocoa samples

The mean of the surface area obtained by the IGC analysis was not significantly different for M1 and M2 (p>0.05), but, the mean value for M3 was significantly different from M1 and M2 (p>0.05).

Table 3.3. Surface area values of cocoa samples obtained by IGC.

	M1	M2	M3
Surface Area by IGC $(m^2/g) \pm$ S.D.	2.82 ± 0.14	2.89 ± 0.11	3.30 ± 0.16

3.4.3 Flowability performance

The aeration test is based on the energy required for the blade to move through the powder by axial forces and rotational torque; the test data are recorded over time. The flow energy (FE) can be calculated using the following equation.

$$FE = \int_{0}^{H} \left(\frac{T}{R \tan \alpha} + F_{base} \right) dH$$

where H is the column height, T is the torque increment, R is the blade radius, α is the helix angle, and F_{base} is the incremental vertical force (Ludwig et al., 2020).

The Aeration test describes the energy required to move a blade across the powder bed. The energy required for the blade to move through the powders helps in understanding the dynamic forces, and inter- and intra-particle interactions.

The aeration profiles of the cocoa powders are presented in Figure 3.5. The flow energy of all cocoa powders substantially decreased when the air velocity increased. The air velocity introduced across the vessel was sufficient for disrupting the particle cohesive forces for the bulk amount of the powders. The data analysis focused on the air velocity value range of 0-6 mm/s. Notably, at the higher air velocity of 6 mm/s, the powders tended to exceed the equipment vessel.
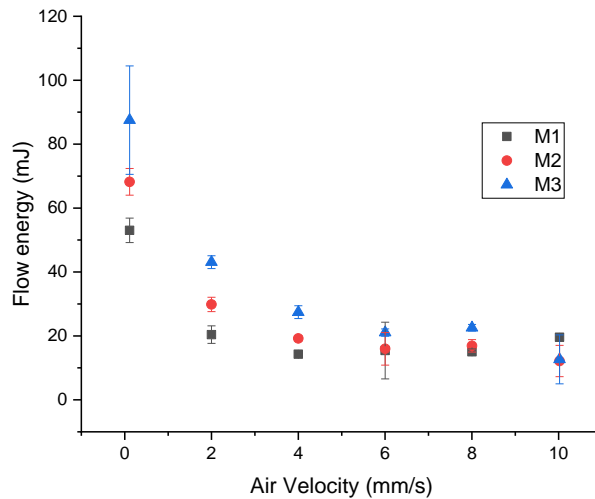
Figure 3.5. Aeration test profile in cocoa powder.

The basic flow energy of aeration at low air velocity is displayed in Figure 3.6. The flow energy for M1, M2, and M3 exhibited a similar tendency at the air velocities of 0.11 and 2.00 mm/s, and statistically significant differences (p<0.05) were observed amongst the cocoa powders. These differences indicate that M3 has higher cohesive force, which makes this powder difficult to fluidize, this observation seems to be as expected because of the higher lipid content at the surface. This relationship for M3 does not seem to apply to the M1 and M2 powders, which

indicates that, under fluidization, the lipid surface content is not the only factor affecting the flow behavior.
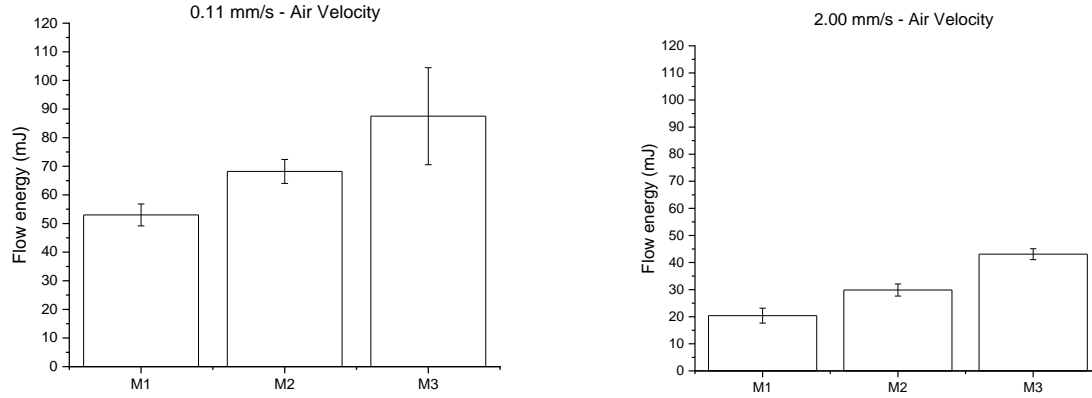
Figure 3.6. Data of basic flow energy of aeration at low air velocity.

The permeability test is based on the measurement of the pressure drop (ΔP) through the powder bed. Darcy's law (Equation 3.1) predicts the movement of a fluid across a powder material as follows (Mohylyuk et al., 2019):

$$Q = \frac{k\,A}{\mu}\frac{P_a - P_b}{L}$$

Equation 3.1

where k is the permeability, Q is the air volume per unit time, A is the cross-sectional area of the powder bed, $P_a - P_b$ is the pressure drop (ΔP), μ is the air viscosity, and L is the length dimension of the powder bed (Mohylyuk et al., 2019).

For Equation 3.1, it is assumed that μ is 1.74×10^{-7} mbar and the flux (q) is equal to Q/A; Equation 3.2 is used in the FT4 calculations.

$$\Delta P = \frac{1.74 * 10^{-7}\,q\,L}{k}$$

Equation 3.2

or

$$k = \frac{1.74 * 10^{-7}\,q\,L}{\Delta P}$$

Equation 3.3

The comparison amongst the permeability of the powders is presented in Fig 3.7. The pressure drop throughout the powder was significantly altered by the applied normal stress. The powder compression steady state was not reached by any of the materials, not even under 15 kPa. Cocoa powders susceptibility for external consolidation stress to induce sintering or caking in the long term may be elucidated with steady state at higher consolidations. Amount of surface lipids, polymorph form and the porosity of the particles affect these instabilities. The length dimension of the powder bed decreased when normal stress was applied, and this increased the bulk density of the powders in the sample's vessel. The permeability (k) and change in pressure ΔP throughout the powder bed is directly related to the length of the powder bed (L). At 15 kPa of applied normal stress, significant differences ($p > 0.05$) were observed in the population means of pressure drop ΔP.
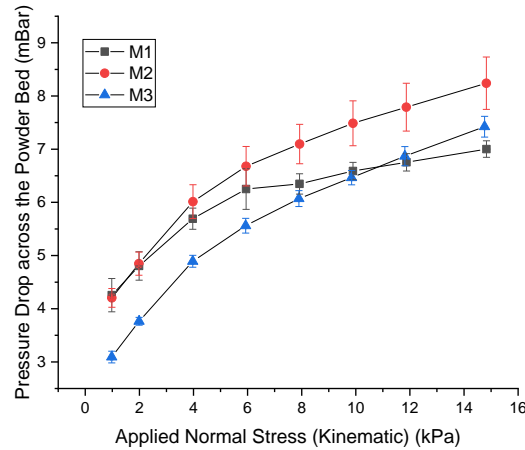
Figure 3.7. Permeability scheme of cocoa samples.

For M1 and M2 powders, the pressure drop was very similar at low applied normal stress. When the applied normal stress increased, response differences were observed. Sample M2 with the lowest lipid content at the surface caused great pressure drop changes throughout the powder, while sample M3 exhibited the lowest pressure drop variation throughout the powder over the range of 0-10 kPa. The obtained results are attributed to the lipid content; Leturia et al. (2014) have

reported similar findings. Moreover, in a previous study, the lipid content in cocoa and cheese products reduced the friction force during the failure planes in a shear cell test (Juliano et al., 2006).

The heterogeneous distribution of fat in cocoa particles, particularly at the surface domain, provides elastic characteristics that confer a non-resistant pathway for the air to pass across the bed system. At higher consolidation normal stresses, in a lipid surface particle, the lipid bridge formation could explain reaching a plateau. To understand the differences in ΔP, normal stresses higher than 15 kPa must be applied in an attempt to explain the material's tendency to form a lipid bridge under a consolidation change.

The permeability behavior results for the three cocoa powders cannot be explained on the basis of fat content. Instead, particle sintering and interlocking forces should be considered. The interlocking forces amongst the particles increase with the applied normal stress and lipid content (Juliano et al., 2006). It has been reported that the cocoa powders are highly compressible, although lipid polymorphism can influence the compressibility, decrease the interaction of surface level forces, and reduce the cohesiveness of cocoa particles (Juliano et al., 2006).

3.4.4   Bulk properties and performance

The aeration behavior responds to the true powder density. The flow energy required to move the blade within the powder bed is less for an air velocity of 2.00 mm/s compared with the initial values at 0.11 mm/s. Powder with low true density is more susceptible to air flow, which facilitates the movement of the stainless-steel blade. In figure 3.8, the true density and surface area appear to be related to the aeration performance of cocoa powders.
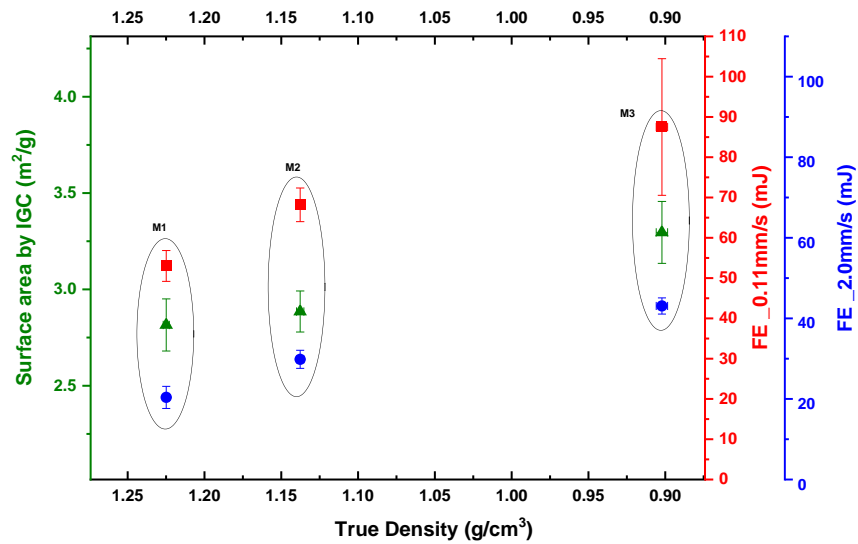
Figure 3.8. Relationship between bulk properties and aeration test.

The permeability results for these cocoa powders are not correlated with the bulk properties, and it remains unclear to what extent the surface fat content affects the viscoelastic deformation. Therefore, it seems that looking at particle morphology of the material, surface roughness and bulk porosity, may contribute to the permeability behavior.

3.5 Conclusions

The flow behavior of cocoa powders was assessed using different methods to understand the powder performance. Although aeration and permeability variations were observed, the powder behavior cannot be explained by any single bulk property. The aeration test differences can be explained by the true density and surface area, but this is not the case for the permeability results.

The findings indicate that the performance of these cocoa powders is likely due to a confounding effect of all variables. The lipid content is different on the cocoa samples and seemed to be responsible for the differences observed in the flow behavior for M1 and M2 samples, because the particle size D_{50} and the mean surface area were very similar (not significantly different). In addition, lipids are vulnerable to slight changes in temperature, triggering the possibility of sintering at higher normal consolidation stresses. Sintering makes the powdered

49

material to coalesce developing particle agglomeration; changing the particle interface roughness, which in turn, increase the interparticle forces among particles. All these variables contribute to the flow behavior of powders containing multiple components, however, the extent of contribution of each variable is hard to quantify and is often is very challenging.

3.6   References

ASTM. (2016). Metal Powder Skeletal Density by Helium or Nitrogen Pycnometry. ASTM B923 – 16

Abrahamsen, A., & Geldart, D. (1980-a). Behaviour of gas-fluidized beds of fine powders part I. Homogeneous Expansion. Powder Technology, 26, 35-46.

Abrahamsen, A., & Geldart, D. (1980-b). Behaviour of gas-fluidized beds of fine powders part II. Voidage of the Dense Phase in Bubbling Beds. Powder Technology, 26, 47-55.

Baerns, M. (1966). Effect of Interparticle Adhesive Forces On Fluidization of Fine Particles. I&EC Fundamentals, 5(4), 508-516.

Duralliu. A., Matejtschuk. P., Williams. D.R. (2019). Measuring the specific surface area (SSA) of freeze-dried biologics using inverse gas chromatography. European Journal of Pharmaceutics and Biopharmaceutics 142, 216–221

Sing, K., Everett, D., Haul, R., Moscou, L., Pierotti, R., Rouquérol, J., Siemieniewska, T. (1985). Reporting Physisorption Data for Gas/Solid Systems with Special Reference to the Determination of Surface Area and Porosity, Pure Appl. Chem. 57, 603.

Fang, T., Tiuz, C., Wu, X., & Dong, S. (1994). Rheological Behaviour of Cocoa Dispersions. Journal of Texture Studies, 26(1995), 203-215.

Juliano, P., Muhunthan, B., & Barbosa-Cánovas, G. (2006). Flow and shear descriptors of preconsolidated food powders. Journal of Food Engineering, 72(2), 157-166.

Lechter, A. (2012). Effect of Minor Components on Cocoa Butter Polymorphism and Kinetics of Crystallization. Cocoa Butter and Related Compounds, AOCS Press, 213-232.

Legras, A., Kondor, Heitzmann, & Truss. (2015). Inverse gas chromatography for natural fibre characterisation: Identification of the critical parameters to determine the Brunauer–Emmett–Teller specific surface area. Journal of Chromatography A, 1425, 273-279.

Leturia, M., Benali, M., Lagarde, S., Ronga, I., Saleh, K. (2014). Characterization of Flow properties of cohesive powders: A comparative study of traditional and new testing methods. Powder Technology, 253, 406-423.

Ludwig, B., Millington-Smith, D., Dattani, R., Adair, J., Posatko, E., Mawby, L., . . . Sills, C. (2020). Evaluation of the hydrodynamic behavior of powders of varying cohesivity in a fluidized bed using the FT4 Powder Rheometer®. Powder Technology, 371, 106-114.

Mohylyuk, V., Styliari, I., Novykov, D., Pikett, R., & Dattani, R. (2019). Assessment of the effect of Cellets' particle size on the flow in a Wurster fluid-bed coater via powder rheology. Journal of Drug Delivery Science and Technology, 54, Journal of Drug Delivery Science and Technology, December 2019, Vol.54.

Tan, J., & Balasubramanian, B. (2017). Particle size measurements and scanning electron microscopy (SEM) of cocoa particles refined/conched by conical and cylindrical roller stone melangers. Journal of Food Engineering, 212, 146-153.

Xie, H. (1997). The role of interparticle forces in the fluidization of fine panicles. Powder Technology, 94, 99-108.

4. WATER UPTAKE ON A LIPID SURFACE PARTICLE SYSTEM

4.1 Abstract

Food systems contain multiple components, including fat located at the surface of particles. Controlling the amount of fat or lipids in food powders can improve the stability of the product. An important quality of food products such as dry powder cocoa-based beverages is their "instant" properties which include wettability, dispersibility and dissolution. Hence, the rehydration of cocoa particles is important for understanding water uptake behavior that governs these instant properties. Water sorption and desorption studies on cocoa particles with different lipid contents at various relative humidities (RH) were performed to determine the diffusion coefficient using Fick's law. Sorption and desorption profiles were similar among the three cocoa powders used in the study, reaching a minimum at 30% RH. The diffusion coefficient results suggest that water diffusion through the particles depends on the hydrophobic surface and internal chemical structure. Surface energetic profiles of the particle microstructure supported the conclusion that a hydrophobic surface, i.e., high lipid content, and high melting points slowed the water uptake kinetics.

4.2 Introduction

Cocoa products, including cocoa beverages and chocolate, are extensively used in the food industry. They are universally consumed and represent a good source of lipids, theobromine, and sugars. These organic compounds contribute to the caloric intake and essential nutrients in the human diet. Cocoa powder is the main ingredient in many beverage formulations, with stabilizers and solubilizers added to enhance the instant properties (Ghosh et al., 2002). The production of cocoa powders involves grinding cocoa nibs after fermentation and drying. When cocoa liquor is produced, a two-phase product is obtained, where solid particles are suspended in a liquid phase enriched with lipids. Subsequently, the cocoa liquor is pressed, wherein the total amount of lipids decreases. Cocoa butter and cocoa cake are obtained separately and cocoa powder is obtained by milling the cocoa cake.

The cocoa powder particle is mainly composed of lipid clusters at the particle surface, whereas cocoa solids are fine particles that concentrate at the core (Vissotto et al., 2010; Do et al., 2011; Vissotto et al., 2014). This is observed during grinding and pressing at high temperature (95-98 °C) and pressure; the high pressure (around 540 bars) (Afoakwa, 2014) and temperature induced the molecular mobility of lipids to the surface; milling produced fine particles 20–40 µm in size with cohesive properties (Figure 4.1).
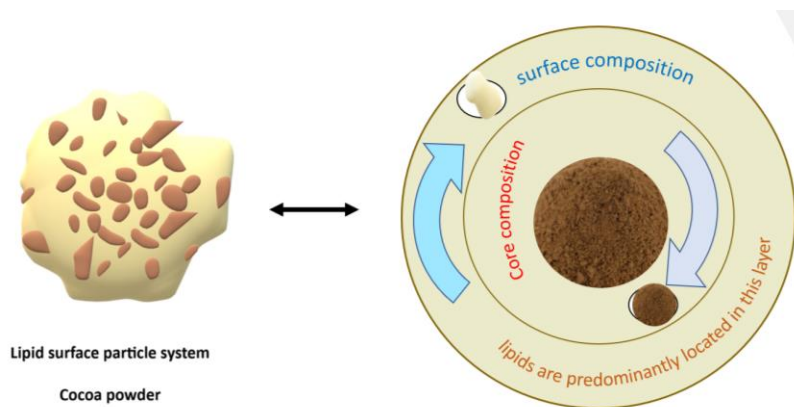
Figure 4.1. Schematic representation of a cocoa particle.

The water content in cocoa powders is commonly used as a quality parameter that must be controlled during processing and storage (Cunningham, 2013). Water exhibits a surface tension higher than the surface energy of cocoa powder, rendering cocoa, with its hydrophobicity, to be not thermodynamically favorable for interaction with water; this significantly affects its wettability (Vu et al., 2003; Kondor & Hogan, 2017; Nnaedozie et al., 2019). The wettability of cocoa powders for beverages with water can be modified using additives (Galet et al., 2004). In the chocolate industry, a commonly used additive in cocoa beverages is lecithin, an emulsifying agent that improves instant properties (Kowalska et al., 2011). This enhanced wettability and dispersibility can be attributed to the increased surface energy of the lecithin–cocoa powder (Galet et al., 2004). Emulsification or dispersion of water–cocoa mixtures improves the particle interactions of hydrophilic and lipophilic substances (Joseph et al., 2019a, 2019b; Wollgorten et al., 2016).

Cocoa particles are complex mixtures that contain multiple components with various physical and chemical properties. A main physical descriptor, particle size by surface-volume

mean, commonly referred to as the Sauter mean diameter, reflects the ratio between the volume to surface area of a circular particle, and is defined by Eq. 4.1. (Kowalczuk & Drzymala, 2016).

$$d_{32} = \frac{\int_{d_{min}}^{d_{max}} d^3 q(d) d\mathrm{d}}{\int_{d_{min}}^{d_{max}} d^2 q(d) d\mathrm{d}} \qquad\qquad 4.1.$$

where $q(d)$ is the diameter frequency distribution, and d_{max} and d_{min} are the maximum and minimum values of $q(d)$, respectively. d_{32} allows identification of an equienergetic point to compare samples and is used for systems with identical surface area, total volume, and surface energy (Kowalczuk & Drzymala, 2016). Herein, the use of the Sauter diameter was selected to obtain meaningful insights regarding the surface-particle size for comparison.

In powders, the diffusion coefficient is used to measure water movement kinetics into each particle. The second Fick's law defines the diffusivity of water through the particle by Eq. 4.2. (Ghosh et al., 2002).

$$\frac{dM}{dt} = D \; \frac{d^2 M}{dx^2} \qquad\qquad 4.2.$$

The coefficient of diffusion is calculated based on the mass change in a boundary condition, and Eq. 4.3 is the solution of Eq. 4.2 for a circumference.

$$\ln\left(1 - \frac{M_t}{M_e}\right) = \ln\left(\frac{6}{\pi^2}\right) - \left[\frac{D\pi^2 t}{r^2}\right] \qquad\qquad 4.3.$$

where M_t is the mass in a specific time, t, during adsorption, M_e is the mass in the equilibrium, r is the particle radius, and D is the diffusion coefficient. The boundary conditions for the calculation fall between the relations of change of the mass being $\frac{M_t}{M_e} > 10\ \%$ and $\frac{M_t}{M_e} < 50\ \%$. In this range, the plot of $\ln\left(1 - \frac{M_t}{M_e}\right)$ vs. t is linear and obeys Fick's law.

Herein, inverse gas chromatography (IGC) was used to investigate the surface energetics of both the hydrophobic, lipidic surface and the fat-free surface of cocoa particles and their role in wettability and kinetics of water penetration through the powder.

4.3   Materials and methods

4.3.1   Materials

Three cocoa powders with different fat contents, Material 1 (M1), Material 2 (M2), and Material 3 (M3), were used. A description of the material origin is provided in Section 3.3.1.

4.3.2   Particle size analysis

A Malvern MasterSizer 3000 (Malvern Instruments Ltd, United Kingdom) was used to measure the particle size via laser scattering. A dry dispersion unit was utilized to obtain particle size measurements.

4.3.3   Surface fat phase extraction

The procedure for surface fat phase extraction was described in Section 3.3.6. For discussion, the extracted fat material will be referred to as non-fat or fat-free to differentiate it from the non-extracted sample, i.e., fat.

4.3.4   Inverse gas chromatography

IGC was used to obtain the surface area of the samples (Section 3.3.7) and surface energetics profiles. The total energetics (γ^T), dispersive (γ^d), and acid-base (γ^{a-b}) surface energy was measured using the SMS-IGC 200 system (Surface Measurement Systems, UK). Six different surface coverages were used to calculate the surface energetics. The surface coverages were chosen depending on the ranges allowed for each solvent, 0.0383, 0.0764, 0.1145, 0.1526, 0.1907, and 0.2288 n/n_m. Approximately 600 mg of the cocoa powder samples were placed inside a pre-salinized glass column with a 1 min control tapping. The dead volume of the column was measured by methane injection at flow rate of 5 cm^3/min. Gas probes, polar and non-polar, were injected into the column to determine the affinity to the powder in the column. A series of non-polar

solvents, alkanes, include hexane, heptane, octane, nonane, and decane, as well as polar solvents ethanol, dichloromethane, ethyl acetate, acetone, and acetonitrile were used. The Schultz method was used to calculate the surface energy components.

4.3.5 Dynamic vapor sorption

Water sorption isotherms were obtained via gravimetric analysis (Model SGA-100, VTI Corporation, USA) and the drying stage was performed at 25 °C until a constant weight was obtained. Relative humidities of 10–90% were used to obtain the sorption properties of the samples, where the equilibrium criterion was set to 0.01% weight change at 25 °C.

4.3.6 Differential scanning calorimetry

Thermal properties were measured by differential scanning calorimetry Q 2000 (TA Instruments, New Castle, DE. USA) with methodology conditions described in Chapter 3.

4.3.7 Statistical Analysis

One-way ANOVA tests were used among samples as a statistical analysis tool. OriginPro, Version 2019b (OriginLab Corporation, Northampton, MA, USA.) and $p < 0.05$ were used to determine significance.

4.4 Results and Discussion

4.4.1 Equienergenetic comparison

The particle size data, described by the mean Sauter diameter, are displayed in Table 4.1. The samples showed a monomodal particle size distribution and the SPAN parameters indicate the width of the distribution, where high span indicates a wide particle size distribution. The mean Sauter diameter for all milled samples ranged from 11 to 13 μm.

Table 4.1. Particle size parameter and surface area of the analyzed cocoa samples (p>0.5).

	M1	M2	M3
D [3,2] µm	12.10 ± 0.37	11.40 ± 0.34	11.73 ± 0.27
SPAN (Dx(90)-Dx(10)/Dx(50))	1.74 ± 0.02	2.79 ± 0.36	2.67 ± 0.06
Surface Area by IGC (m^2/g)	2.82 ± 0.14	2.89 ± 0.11	3.30 ± 0.16

The surface area (Table 4.1) was determined by adsorption of ethanol and infinite dilution by IGC. The SA values were similar for M1 and M2 and lower than that of M3, M3 is significantly different (p>0.5) for M1 and M2 samples.

Table 4.2. Total surface energetics values at 0.2288 surface coverage.

	M1	M2	M3
Total surface energy (mJ/m^2) at 0.2288 coverage	42.92	42.22	43.68

For materials to have a point of equienergetic comparison, the surface energy should not be significantly different (Kowalczuk & Drzymala, 2016). Table 4.2 shows that the value of total surface energy for all materials ranged from 42 to 44 mJ/m^2 at a surface coverage of 0.2288. This coverage was chosen to ensure that physisorption occurred during the interaction between the gas probe and powders. A plateau was reached at approximately 0.22 of surface coverage (Figure 4.3), and values above 0.22 showed the same energetic magnitudes (Williams, 2015).

The data from these cocoa properties suggested that these powders M1 and M2 are equienergetic as shown in Table 4.2. In addition, to the similar surface energy range values, the surface area was also similar but the particle size was slightly different. Interestingly, M3 particle size is not significant different among powders, but the surface area and surface energetics are significantly different from M1 and M2. This information is going to be relevant for the explanations provided below.

4.4.2   Surface energetics

As mentioned previously, the multiple components in cacao particles are distributed in a non-uniform manner. Fat, the major component of interest, is located on the surface and in the core. Upon fat extraction from the cacao surface, the total fat content was reduced, leaving fat in the core. The extracted amount of lipids was different for all three samples (Figure 4.2), where the sample M3 exhibited higher fat content than the M1 and M2 samples.
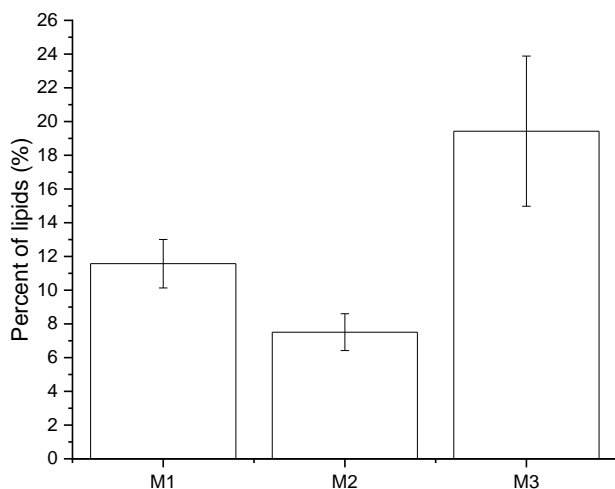
Figure 4.2. Lipid contents in the cocoa samples.

The physisorption of non-polar and polar probe molecules on the surface allows for the determination of dispersive and acid–base components, respectively (Ho, R et al., 2012; Willians et al., 2015). The surface chemistry heterogeneity was evaluated by measuring the surface energy profiles at six different surface coverages for samples with and without fat on the surface.

The surface energetics profiles are displayed in Figures 4.3 and 4.4 for powders containing fat (as-received samples) and without fat (fat extraction), respectively. At a low surface coverage, infinite dilution principles apply, while the probe molecules were assumed to interact only with active sites on the particle. Therefore, particle interactions are stronger and high surface free energies are expected (Ho, R et al., 2012).

The surface energetics, at surface coverages of 0.05–0.25 n/nm, for samples with fat ranged between 42–46 and 40–45 mJ/m^2 for total and dispersive components, respectively. The surface energetics, at the same surface coverage range (0.05–0.25 n/nm), for the non-fat samples (fat extracted) were 40–45 and 35–40 mJ/m^2, for the total and dispersive components, respectively.
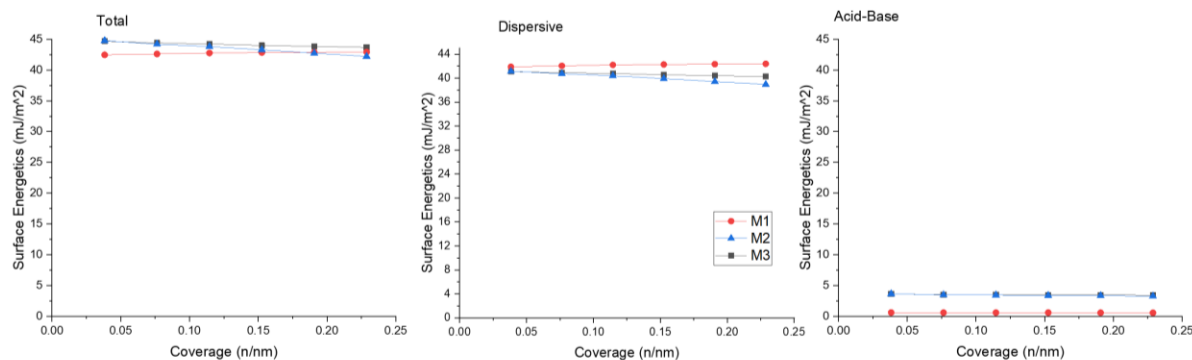
Figure 4.3. Surface energetic profiles of the as-received samples and fat at the surface.

The total surface energetics (γ^T) for the fat and non-fat samples were very similar. The dispersive component of surface energy (γ^d) reflects the hydrophobic character; the γ^d for the fat samples was 40–45 mJ/m^2 while that of the non-fat samples was 35–40 mJ/m^2. Clearly, γ^d displayed higher value for the lipid-rich surface than for the lipid-starved surface, suggesting the overall surface interactions, cocoa-cocoa or cocoa-water, are more favorable for fat-containing samples. In this regard, surface properties have an impact on the interactions of dry cocoa powders, and on the reconstitution of cocoa-based products. The instant properties (wettability, dispersibility and dissolution) depend on both the surface and microstructural characteristics of the particles.
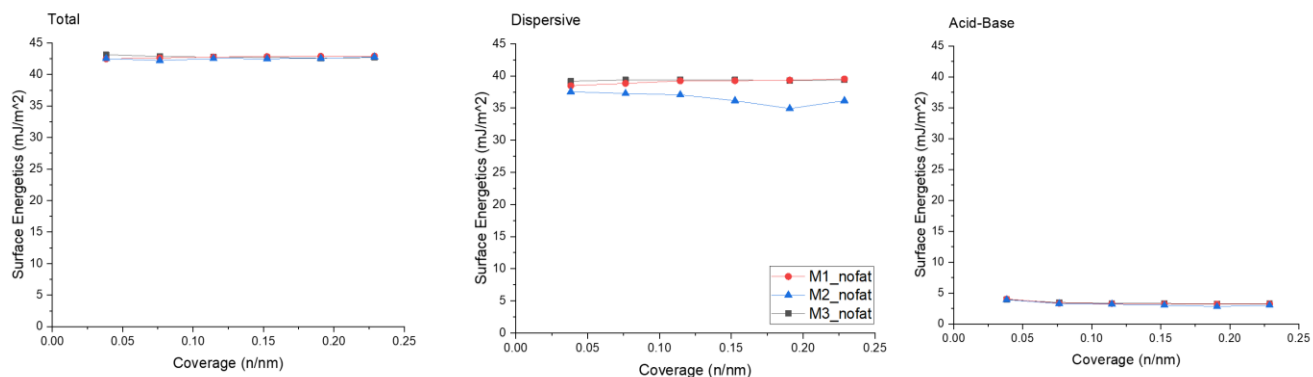
Figure 4.4. Surface energetic profiles for the samples with lipids and lipid-extracted (non-fat).

Surface energetics for the components of the non-fat samples are listed in Table 4.3. The acid–base component of the surface energy (γ^{a-b}) for M1 was 0.55 mJ/m². Conversely, the γ^d for M1 was 42.37 mJ/m², and was the highest among the samples tested, where non-polar interactions were predominant.

Table 4.3. Components of the surface energy of non-fat extracted samples.

	M1	M2	M3
Dispersive surface energy (mJ/m²) at 0.2288 coverage	42.37	38.95	40.26
Acid–base surface energy (mJ/m²) at 0.2288 coverage	0.55	3.26	3.42

.

Figure 4.5 shows the specific acid–base free energy distribution obtained using ethanol as a probe molecule. The SEA analysis software calculated the area under the curve in the surface coverage plot figure 4.3. The surface energy distribution obtained using ethanol increases understanding of the water sorption, as an ethanol is a polar probe. The information in figure 4.5 is only displayed for surface heterogeneity comparisons.
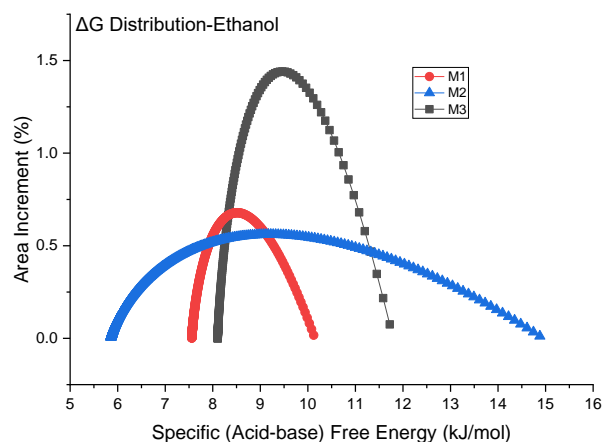
Figure 4.5. Specific (acid–base) free energy obtained using ethanol (polar probe) with the 'area under the curve' method for six surface coverages on the as-received samples.

The information in Figure 4.5 displays detailed energetic profile distributions of the surface that represent the heterogeneity among the three samples. The surface energy distributions of the samples represent the availability of energy sites that contribute to interactions. Narrow distributions for the M1 and M3 powders suggest less heterogeneous active sites compared to the M2 powder. The uniformity of M3 showed narrow uniformity distribution suggesting more specific available energetic sites expressed in the percentage of the overall contribution. This represents high affinity for the polar (ethanol) vapor molecules per unit of surface area at 9.5–10.5 kJ/mol, M1 has fewer active sites per unit surface area with a maximum of 0.7% of area increment at around at 8–9 kJ/mol. The broad energetic distribution of the M2 powder refers to highly heterogenic active sites in the range 6–15 kJ/mol for polar (ethanol) interactions.

4.4.3 Thermal properties and polymorphism in the cocoa samples

Each cacao material showed different onset temperatures (Table 4.5) of the polymorphic transformations that may occur during grinding of the cocoa cake. From the DSC thermograms (Figure 4.6), the onset temperatures were determined (Table 4.5). Subsequently, when the samples were tested using a cooling step methodology, the M1 and M2 powders showed polymorphic transformations. The polymorphs onset measurement for M3 exhibited melting points of 26.96

and 30.97 °C (Table 4.5), corresponding to highly energetic polymorphs, β'_1 and β_2 (Table 2.1 in chapter 2) (Afoakwa, 2014), respectively, mainly due to the packing structure.

Table 4.4. Thermal physical transition properties of the as-received samples.

	First onset (°C)	Second onset (°C)	Peak temperature (°C)	Enthalpy (ΔH_f) normalized (kJ/g)
M1	22.67	26.17	30.32	16.307
M2	21.47	25.36	30.03	11.979
M3	26.96	30.97	33.12	16.860

The enthalpies of fusion (ΔH_f) were different for all three samples and the ΔH_f for M1 and M3 were lower than that of M2, which could be attributed to the low lipid content. Table 4.5 lists the two onset temperatures for each sample, indicating the existence of multiple polymorphs in the cocoa particle.

Polymorph onsets are visible in the DSC heating thermogram, and the differences between the as-received samples with sample subjected to cooling show shifts in the onsets and distinction between peak maxima.
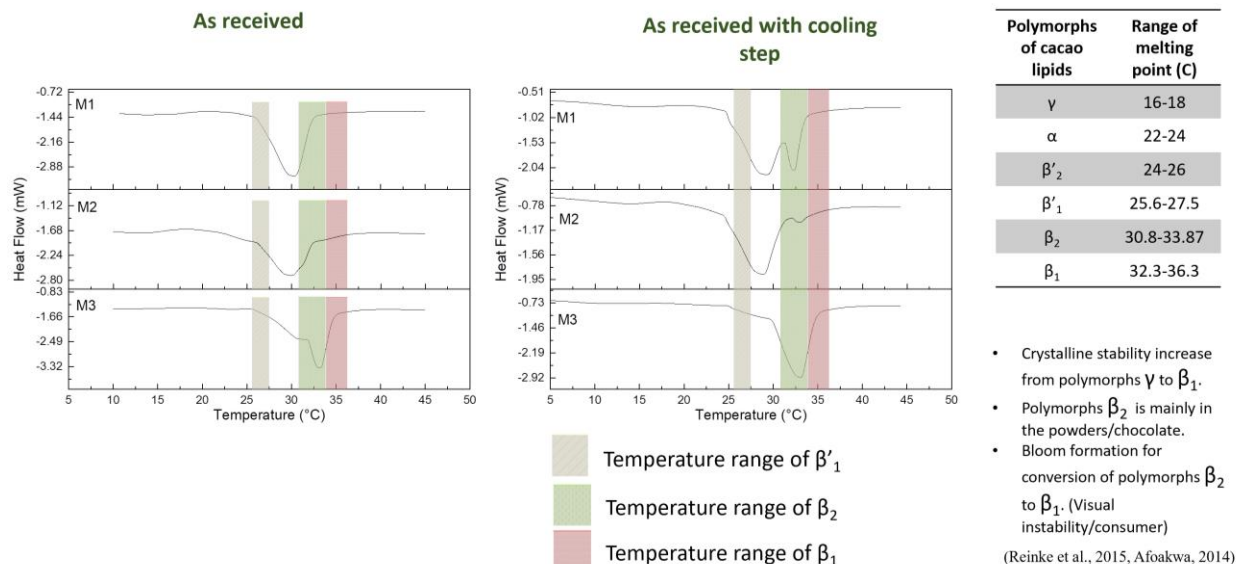
Figure 4.6. Thermal properties of the cocoa samples measured by DSC.

Samples were subjected to a cooling stage at –10 °C for 10 min. The analysis results showed that the cooling step generates changes and increases the number of melting onsets, especially in the M1 and M2 samples (Table 4.6). Sample M1 showed four onset temperatures α, β'$_2$, β'$_1$, and β$_1$; M2 displayed three α, , β'$_1$, and β$_1$; and M3 exhibited two polymorphs, β'$_1$ and β$_2$. The fact that the M1 and M2 samples contained various polymorphs, they are expected to be highly unstable at temperatures of >30 °C. The data indicated the importance of controlling the temperature during processing. Tempering can be considered as an approach to improve the stability for M1 and M2 during grinding, if it can form the β$_1$ polymorph. The conversion of polymorphs due to changes in temperature history destabilizes the cocoa powder (Petit et al., 2017).

Table 4.5. Thermal physical transition properties of the as-received samples processed with a cooling step.

	Onset (°C)	Enthalpy of melting (ΔH_f) normalized (kJ/g)
M1	First: 22.82 Second: 24.45 Third: 26.66 Fourth: 31.42	18.194
M2	First: 22.97 Second: 24.15 Third: 32.18	12.109
M3	First: 24.94 Second: 29.36	18.063

4.4.4 Sorption isotherms and diffusion coefficients

The sorption isotherms results are very similar across samples, without apparent differences in the water uptake or wettability (Figure 4.7.) All powders exhibited a type II isotherm (Medeiros et al., 2006). Figure 4.7a revealed three regions in the isotherm curve, I (0–20% RH), II (20–40% RH), and III (40–80% RH). Region I involves the beginning of adsorption of water on the powder bed; Region II represents the region of a monolayer and further to conversion to multilayer formation on the surface; and in Region III, more layers are formed due to condensation and saturation of water molecules. The hysteresis after desorption represents water molecular mobility inside the particle and retention ability of the particles. Figure 4.7b represent the region I and II and the inflection point where a monolayer total surface coverage was reached.
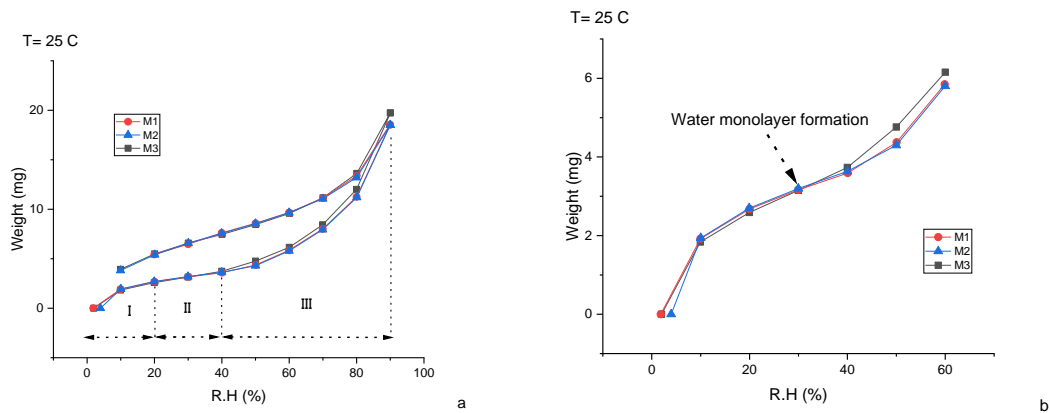
Figure 4.7. a. Sorption/desorption isotherms of cocoa samples, b. Relative humidity of the point of a monolayer formation.

Using diffusion coefficients, it is possible to determine differences in water diffusion kinetics through the cocoa powders. The diffusion coefficient was measured at different relative humidities. At low RH, the water molecules first interact with the particle surface with hydrophobic character and high lipid content. As RH increases, the water molecules diffuse inside the particle structure and mass transfer occurs.
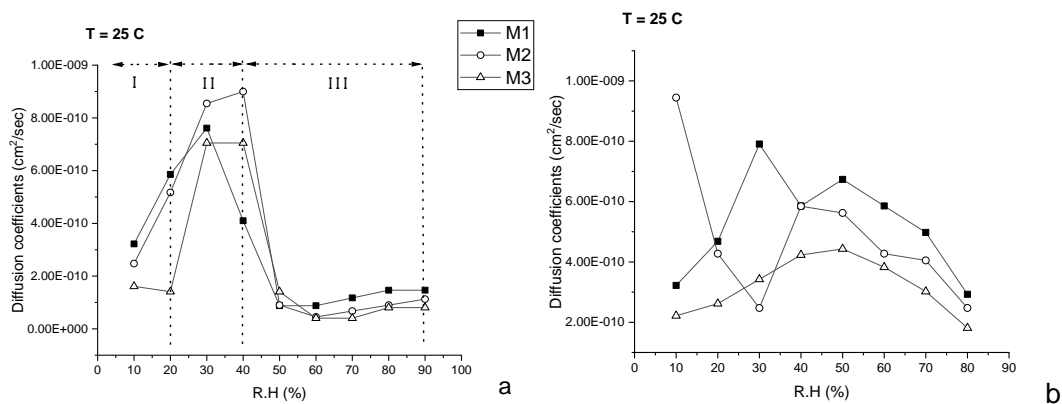
Figure 4.8. Diffusion coefficients over a range of relative humidity: (a) sorption and (b) desorption.

In Figure 4.8a, the M3 sample contained the highest lipid content and lowest diffusion coefficient at 10–40% RH (Region I and II) compared to the other cacao powders. All samples exhibited a dramatically decreased diffusion coefficient at ≥40% RH (Region III). Thus, water surface affinity can be discussed from an energetics standpoint in Section 4.4.5. Figure 4.8 b shows the desorption behavior was similar among all samples. The diffusion coefficient increases from 80% to 50% RH and overall decreases between 50% to 10%. Although, it is particular interesting to notice the diffusion coefficient in the desorption process drop for minimum value for M2 at 30% RH (Figure 4.8b), lower humidifies induce changes in the water particle affinity.

4.4.5   Water diffusion coefficients as a function of surface energetics

The water sorption isotherms of powdered materials depend on their nature and composition. The cocoa powders exhibited similar particle sizes and surface areas; thus, the affinity for water was driven by the surface energy and composition. The water sorption isotherms seemed independent of composition in terms of fat content. The diffusion coefficient offers deeper insight in the microstructure of the cocoa powder matrix. At low RH values, water vapor adsorbs into the powder and significant increase in diffusion coefficient was observed. At RH ≥50%, saturation condensation or liquid diffusion may occur, reaching a similar plateau for all three samples.

The water mobility reached at maximum at 30–40% RH, which can be explained in terms of surface energetics (Fig. 4.9). The maximum diffusion coefficient was observed after a water monolayer was formed on the particles, where the surface energy of the particle should be close the water surface tension. The surface is in principle lipophilic, but a water monolayer was created at 30% RH, whereas at ≥40% RH, the diffusion coefficient reached equilibrium and considerably dropped by approximately five times for all powders.
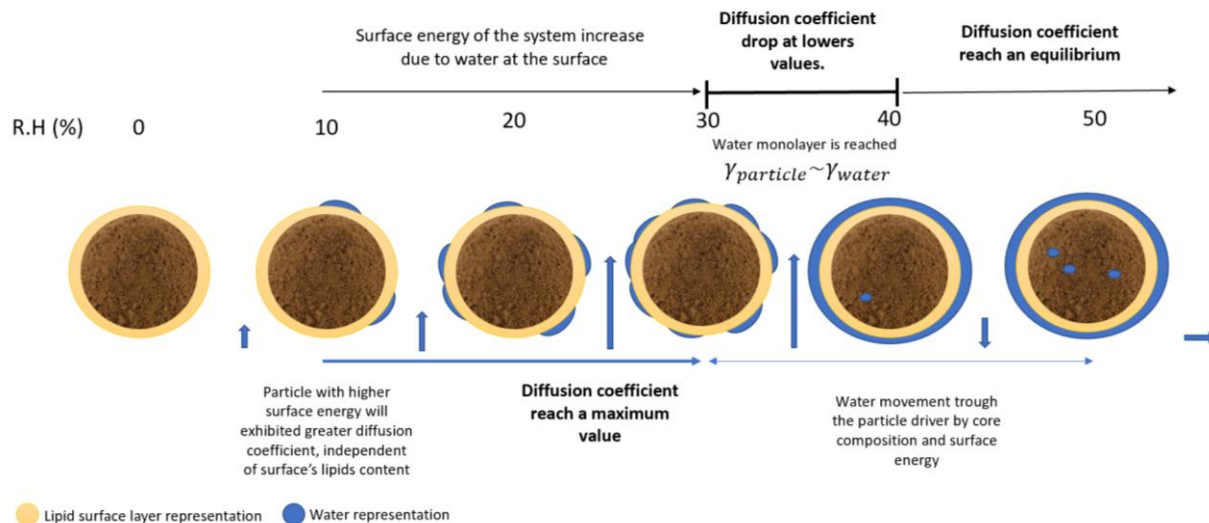
Figure 4.9. Schematic of the water sorption mechanism in a lipid surface particle system.

During desorption, the diffusion coefficient at 80–50% RH was governed by the core structure, with water movement from the core to particle surface. Differences in diffusion coefficient of desorption among samples were significant (Figure 4.8b), core chemical composition affect the affinity for water to the internal structure, while surface and core composition differ, a chemical core-surface gradient explain the differences in the kinetic of diffusion. M1 exhibited the highest desorption diffusion coefficient, but no strong trend was observed in terms of lipid content.

The energy profile of the acid–base component for the M3 powder showed a high value of specific surface energy 3.30 mJ/m^2, suggesting high affinity for water. The water mobility on the powder surface may depend on the lipid polymorph. Polymorphs have different crystal packing in the unit cell, with the results, it is hypothesized that polymorphs impact water mobility in the microstructure. Measuring the water coefficient diffusion at 25 °C may cause lipid physical transformation, and the water mobility depends on polymorph packing, imparting a high affinity to water. M1 and M2 contained less packed polymorphs compared to M3.

The lipid contents were calculated to examine the potential correlation of the surface lipid contents with water sorption properties, and the associated impacts on the diffusion coefficient. The mobility of water on the powder surface could depend on the polymorph instead of other powder physicochemical properties. It was clear that powders with lower onsets (M1 and M2)

exhibited higher diffusion coefficients at 10 to 40% RH, and higher desorption from 80 to 40% RH. This study explains the water adsorption phenomenon from a surface energetics standpoint, and a mechanism was proposed to understand the significant drop in diffusion coefficient after 40% RH in lipid surface particle systems. Water diffusion coefficients at different RHs were not dependent on the lipid content in the particles.

4.5   Conclusions

A mechanism was proposed based on the surface energy contributions of the particles. Chemical compositional differences between the core and the surface particle structure create a chemical gradient that affect the water diffusion. Surface heterogeneity, measured to polar solvent (Ethanol), were evident among particles. Water sorption isotherms were insufficient to distinguish water–cocoa powder interactions among the cocoa powders studied herein. The diffusion coefficient of sorption profile at 10–90% RH showed differences in diffusion as follows: 1) At 0–20% RH, the diffusion coefficient of vapor water increased; 2) At 20–40% RH, another adsorption step was observed, reaching saturation; 3) At 40–90% RH, saturation occurred, switching to absorption of liquid water. The formation of a water monolayer influenced further water diffusion at higher RH, representing a boundary for surface diffusion control. The complementary explanation for the diffusion results at the molecular level involves the change of particle surface energetics over the range of RH tested herein. Whereas desorption showed differentiation of the powders due to hysteresis from 90 to 50% RH, the internal structure of the M3 powder showed higher water affinity. A diffusion mechanism is proposed and it serves the purpose of understanding the water affinity behavior of complex food products, where the food product must present a considerable lipid content located at the surface for quality and consumer acceptance. Core composition also influences the kinetics of diffusion, a chemical gradient permits it to be thermodynamically posible. The IGC technique offers a detailed energetic profile of the surface and provides the necessary means to assess changes in surface energy over a range of RH.

4.6   References

ASTM. (2013). Standard Test Methods for Water Vapor Transmission of Materials. ASTM E96 / E96M – 13

Afoakwa, E.O. (2014). Cocoa processing technology. CRC Press: Taylor & Francis Group, pp. 179-180.

Cunningham, W. (2013). Use of water activity characteristics enables a simplified approach for defining the reference moisture condition for FDA cocoa powder in-house reference material. Analytical and Bioanalytical Chemistry, 405(26), 8615-8620.

Do, T., Vieira, J., Hargreaves, J., Mitchell, J., & Wolf, B. (2011). Structural characteristics of cocoa particles and their effect on the viscosity of reduced fat chocolate. LWT - Food Science and Technology, 44(4), 1207-1211.

Petit, J., Michaux, F., Jacquot, C., Chavez, E., Dupas, J., Girard, V., Gianfrancesco. A., Scher. J., Gaiani, C. (2017). Storage-induced caking of cocoa powder. 199, 42-53.

Galet, L., Vu, T., Oulahna, D., & Fages, J. (2004). The wetting behaviour and dispersion rate of cocoa powder in water. Food and Bioproducts Processing, 82(4 C), 298-303.

Ghosh, V., Ziegler, G., & Anantheswaran, R. (2002). Fat, moisture, and ethanol migration through chocolates and confectionary coatings. Critical Reviews in Food Science and Nutrition, 42(6), 583-626.

Ho, R., Dilworth, S., Williams, D., & Heng, J. (2011). Role of Surface Chemistry and Energetics in High Shear Wet Granulation. 9642-9649.

Ho, R., Naderi, M., Heng, J., Williams, D., Thielmann, F., Bouza, P., . . . Burnett, D. (2012). Effect of Milling on Particle Shape and Surface Energy Heterogeneity of Needle-Shaped Crystals. 2806-2816.

Joseph, C., Savoire, R., Harscoat-Schiavo, C., Pintori, D., Monteil, J., Faure, C., & Leal-Calderon, F. (2019a). Redispersible dry emulsions stabilized by plant material: Rapeseed press-cake or cocoa powder. Lwt, 113(June), 108311.

Joseph, C., Savoire, R., Harscoat-Schiavo, C., Pintori, D., Monteil, J., Leal-Calderon, F., & Faure, C. (2019b). O/W Pickering emulsions stabilized by cocoa powder: Role of the emulsification process and of composition parameters. Food Research International, 116(May 2018), 755-766.

Kondor, A., & Hogan, S. (2017). Relationships between surface energy analysis and functional characteristics of dairy powders. Food Chemistry, 237, 1155-1162.

Kowalczuk, P., & Drzymala, J. (2016). Physical meaning of the Sauter mean diameter of spherical particulate matter. Particulate Science and Technology, 34(6), 645-647.

Kowalska, J., Majewska, E., & Lenart, A. (2011). Sorption properties of a modified powdered cocoa beverage. Chemical and Process Engineering - Inzynieria Chemiczna i Procesowa, 32(1), 21-31.

Medeiros, M., Ayrosa, A., De Moraes Pitombo, R., & Da Silva Lannes, S. (2006). Sorption isotherms of cocoa and cupuassu products. Journal of Food Engineering, 73(4), 402-406.

Nnaedozie, C., Sanders, C., Montes, E., Forny, L., Niederreiter, G., Palzer, S., & Salman, A. (2019). Investigation of rehydration of food powder mixtures. Powder Technology, 353, 311-319.

Reinke, S., Roth, S., Santoro, G., Heinrich, S., & Palzer, S. (2015). Tracking Structural Changes in Lipid-based Multicomponent Food Materials due to Oil Migration by Microfocus Small-Angle X - ray Scattering. ACS Appl. Mater. Interfaces, 9929-9936.

Vissotto, F., Giarola, R., Jorge, L., Makita, G., Cardozo, G., Rodrigues, M., & Menegalli, F. (2015). Morphological characterization with image analysis of cocoa beverage powder agglomerated with steam. Food Science and Technology, 34(4), 649-656.

Vissotto, F., Jorge, L., Makita, G., Rodrigues, M., & Menegalli, F. (2010). Influence of the process parameters and sugar granulometry on cocoa beverage powder steam agglomeration. Journal of Food Engineering, 97(3), 283-291.

Vu, T., Galet, L., Fages, J., & Oulahna, D. (2003). Improving the dispersion kinetics of a cocoa powder by size enlargement. Powder Technology, 130(1-3), 400-406.

Williams, D. (2015). Particle Engineering in Pharmaceutical Solids Processing: Surface Energy Considerations. Current Pharmaceutical Design, 21(19), 2677-2694.

Wollgarten, S., Yuce, C., Koos, E., & Willenbacher, N. (2016). Tailoring flow behavior and texture of water based cocoa suspensions. Food Hydrocolloids, 52, 167-174.

5. THERMODYNAMICS AND SURFACE PROPERTIES OF COCOA POWDERS

5.1 Abstract

In this study, the thermodynamic properties of cocoa powder systems were investigated based on surface characterization methodology. It is important to understand the effect of temperature fluctuations during processing on the surface of the cocoa powders. The surface properties associated with cocoa powders include surface chemistry compositional variations, particle interactions and particle morphology changes, as well as phase transitions, all in turn, affect the quality of the cocoa-based beverages. The cocoa particles contain multiple constituents, with those at the surface, such as lipids are of particular interest. The physical state of these lipids impacts the cohesive and adhesive interactions of particles leading to caking, flowability, agglomeration and stickiness. In this research, particle surface characterization addresses the susceptibility of lipids to temperatures that influence water sorption and interactions. Various surface analytical methods were developed to address the thermodynamic parameters, these were probed using inverse gas chromatography (IGC), the enthalpy of sorption assessed the surface affinity with *n*-heptane under isosteric conditions while the melting point transition evaluated lipid phase transformations. The sorption isotherms were used for determining the water diffusion coefficients at three temperatures using dynamic vapor sorption (DVS), and the activation energies of diffusion were fitted into the Arrhenius-type equation. The surface of the cocoa matrix was evaluated by X-ray photoelectron spectroscopy (XPS) to distinguish chemical surfaces species. The results revealed the vulnerability of the cocoa powders to temperature changes. The M1 sample was characterized by the initiation of lipid melting at the surface; the M2 sample exhibited the highest sorption enthalpy, indicating the strongest molecular surface interactions with the *n*-heptane among of the powders. This thermodynamic study shows the importance of the surface approach for understanding powder performance in order to improve the stability of cocoa powder systems.

5.2 Introduction

Surface properties are not included in the stability protocols for evaluating powder food products. The lipids at the surface affect particle interaction and powder performance (Jacquot et al., 2016). Crucially, the lipid phase is susceptible to melting and polymorphic transformations when the temperature changes. The cocoa industry regularly encounters issues in cocoa powder production, as pointed out in chapter one. Cocoa powder instability is attributed to particle-particle interactions, promoting agglomeration and losses during production. Modifications of the cocoa matrix, such as alkalization or lecithination, have produced beneficial outcomes in cocoa beverages production (Selamat et al., 1998).

Chemical characterization techniques for food powders based on the surface are important for differentiating the core from the outer particle composition (Murrieta-pazos et al., 2012). Generally, the particles in the cocoa powders, with high amounts or low-melting-point lipids, commonly form fat bridges, for example, upon storage (Burgain et al., 2017). Differential scanning calorimetry (DSC), a thermal technique, is used to detect the onset of the melting point without distinguishing the core–surface interparticle transition. Conversely, inverse gas chromatography (IGC) has been employed for quantifying the surface glass transition temperature and melting point in pharmaceuticals and polymers, respectively (Otte & Carvajal, 2011; Fernandez-Sanchez et al., 1991). However, the IGC has not been used for complex food mixtures, in this case, to measure phase transitions for lipids at the surface. In fact, the surface microstructure evolution due to temperature must be considered to improve the stability of dry powders in compositionally complex powder systems.

The IGC involves a configuration suitable for achieving solid-gas phase equilibrium in a specific experimental condition. The Clausius-Clapeyron equation relates the two-phase equilibrium (Levine, 2009) as follows:

$$\frac{dP}{dT} = \frac{\Delta H_m}{T \, \Delta V_m} = \frac{\Delta H}{T \, \Delta V} \qquad \text{Equation 5.1.}$$

where P is the pressure, T is the temperature, ΔH_m is the molar enthalpy of the process, and ΔV_m indicates the molar volume change. For the IGC configuration, at the infinite dilution setting, the probe molecule is assumed to follow the ideal gas regimen expressed as

$$P \approx \frac{RT}{\Delta V_m} \: or \: \Delta V_m \approx \frac{RT}{P} \qquad \text{Equation 5.2.}$$

Therefore, for the IGC, the Clapeyron equation is (Onjia & Nastasovi, 2008) restated as

$$\frac{d \ln V}{dT} \approx \frac{\Delta H_m}{RT^2} \qquad \text{Equation 5.3.}$$

Likewise, since $d(1/T) = -(1/T^2) dT$ (Levine, I. 2009), the previous equation can be written as

$$\frac{d \ln V}{d(1/T)} \approx \frac{-\Delta H_m}{R} \qquad \text{Equation 5.4.}$$

Further, for the IGC, the volume is measured from the sorbate retention time, and this is termed the net retention volume Vg, and so, equation 5.4 is transformed to (Onjia & Nastasovi, 2008)

$$\frac{d \ln V_g}{d(1/T)} \approx \frac{-\Delta H}{R} \qquad \text{Equation 5.5.}$$

During a phase transition, the solid phase and gas probe molecules interact, causing retention volume changes. For the IGC plotting $\ln V_g$ vs (1/T) produces a Z-shaped retention diagram. Detailed descriptions of the transition diagram from the IGC are provided in (Onjia & Nastasovi, 2008) and (Otte & Carvajal, 2011), with a straight line indicating no phase transition. Considering the surface coverage (θ), equation 5.6 is suitable for calculating the isosteric sorption enthalpy.

$$\left(\frac{d \ln V_g}{d\left(\frac{1}{T}\right)} \right)_\theta \approx \frac{-\Delta H}{R} \qquad \text{Equation 5.6.}$$

Onjia & Nastasovi (2008) calculated ΔH using equation 5.5, and proposed it to be termed the enthalpy of sorption before the system attains the T_g, and enthalpy of mixing thereafter. For

the first, physisorption is assumed as the primary interaction in the solid–gas system. After achieving the T_g, the gas molecules interact stronger with the solid phase at the surface, and to some extent in the bulk. For the cocoa system, the interactions are limited to surface physisorption, since the glass transition temperature phenomenon is absent, and so, the term enthalpy of mixing is unnecessary for the cocoa system.

In surface particle–water interactions, most studies focus on producing sorption isotherms, primarily, to assess the water uptake for a relative humidity range. However, when the kinetics of water diffusion is more relevant, water–sorption isotherms are useful for obtaining diffusion coefficients and determining the Arrhenius activation energies. Predicting the water absorption susceptibility of powders and understanding the kinetics of the water movement through the solid is useful (Fiorentini et al., 2015). Initially, Arrhenius developed the equation relating the reaction rate (k) and the temperature as follows (Levine, 2009):

$$k = Ae^{-E_a/RT}$$ Equation 5.7.

where A is a constant parameter, E_a is the activation energy, T is the temperature, and R is the gas constant, with a value of 8.314 J K^{-1} mol^{-1}. The Arrhenius equation has been applied to unconventional phenomena including the chirping of tree crickets, creeping of ants, flashing of fireflies, rate of terrapin heartbeat, and alpha brainwave frequencies (Laidler, 2019). In the pharmaceutical field, the Arrhenius activation energy is widely applied and satisfactorily used for accelerated studies at variable temperatures to predict the shelf life of drug substances and their products.

The diffusion coefficient displays a temperature dependence that is predictable by the Arrhenius equation (Chvoj, 1999). If the E_a is independent of the temperature, the integration of equation 5.7 produces the expression (Levine, 2009)

$$\frac{d\ln K}{dT} = \frac{E_a}{RT^2}$$ Equation 5.8.

To calculate the diffusion coefficient, equation 5.7 is transformed as follows:

$$D(T) = Ae^{-E_d/RT}$$ Equation 5.9.

74

where D is the temperature-dependent diffusion coefficient, if A and E_d are constant. By considering the natural logarithm of Equation 5.9, the following expression is obtained

$$\ln D = lnA - \frac{E_d}{RT} \qquad \text{Equation 5.10.}$$

Following the Arrhenius approach for the diffusion coefficient analysis, plotting 1/T versus ln D produces a slope for calculating the E_d according to the relationship:

$$\text{Slop}e = -E_d/R \qquad \text{Equation 5.11}$$

Thus, the activation energy of a reaction in terms of diffusion coefficient is defined as the minimum energy required for the water molecules to initiate diffusion through the solid particles (Levine, 2009).

When a solid is involved in adsorption, two types of gas-solid interactions include: 1) physical adsorption (physisorption) and 2) chemical adsorption (chemisorption). In a physisorption event, weak intermolecular forces like the van der Waals are exhibited, whereas for chemisorption stronger chemical interactions and molecular bonding (e.g., covalent) are present. The thermodynamic parameters measured by the IGC and the dynamic vapor sorption (DVS) can reveal particle-gas interactions, particle-particle affinities, and water-particle interactions useful for stability assessment.

The aim of this study was to determine the thermodynamic properties of cocoa powder systems by using surface characterization techniques. The stability of cocoa powders may be predicted from the enthalpy of sorption; hence, a probe molecule with high affinity and appropriate interaction is selected to differentiate the transition temperatures for predicting the flowability and caking instabilities among the samples. Moreover, the diffusion activation energy may serve in predicting the rate of water movement from the surface to the core of particles at different temperatures indicating which powders are liable or susceptible to instability in the long term. In this study, the possibility of using the IGC under isosteric conditions or DVS to assess enthalpy of sorption and the diffusion coefficient is highlighted, respectively.

5.3   Materials and Methods

5.3.1   Materials

Three cocoa powders termed Material 1 (M1), Material 2 (M2), and Material 3 (M3), with different fat (lipid) contents were used in the experiments (as in Chapter four). M1 and M2 samples were obtained from the same manufacturer (A) that used the same procedure with the only difference between the two lots was in the fat content: whereas M3 sample was obtained from company B and produced under different conditions.

5.3.2   X-ray photoelectron spectroscopy (XPS) measurements

A Kratos Ultra DLD (Manchester, UK) instrument was used to obtain the XPS spectra with an Al Kα source (hν = 1486.58 eV) operated at 160 eV. Quantification with the survey spectra was carried out in Casa XPS software, which defined peaks regions of energy. The atomic concentration was computed using the predefined relative sensitivity factor (RSF) for each element, following the Shirley and Tougaard methods utilized for background corrections.

5.3.3   Phase transition by inverse gas chromatography

Approximately 600–620 mg of the cocoa powder sample was filled in a silane-treated column of length 30 cm and internal diameter 4 mm. A non-polar hydrophobic adsorbate, *n*-heptane, was injected into the IGC by using a single pulse with a carrier gas flow of 10 cm^3/min. Isosteric conditions at 0.2 surface coverage were maintained over the temperature range from 20 °C and 40 °C, representing the minimum and maximum temperatures, respectively, allowed by the equipment. The reasons for choosing *n*-heptane as the adsorbate are: 1) its molecular affinity with cocoa lipids and 2) its short retention time of 2–8 min in every pulse, that enables sample analysis in 2–3 hours. The samples were analyzed as received, without preconditioning, since cocoa lipids in the powder can be affected by any preconditioning temperature.

The data from the chromatograms were used to calculate the minimum phase transition temperature and the sorption enthalpy. The columns were prepared for each run, with 3 columns utilized per sample. The re-use of a filled column is unadvisable because of irreversible changes in the sample surface structure caused by temperature. The Surface Energy Analyzer Software

Advanced version 1.4.1.0 was used for calculating the phase transition temperature. The raw data were collected and used to calculate the sorption enthalpy using equation 5.6.

5.3.4 Activation energy of diffusion from dynamic vapor sorption

The water sorption isotherms were obtained in the relative humidity (RH) range 10–90% using 5–6 mg of sample placed in a quartz sample holder. A gravimetric equipment (Model SGA-100, VTI Corporation, USA) was used to obtain isotherms at 25, 30, and 35 °C; an equilibrium criterion of 0.01% was used as the boundary between the changes in RH. The activation energy of diffusion E_{ad} was then calculated using the Arrhenius equation.

5.4   Results and Discussion

5.4.1   Chemical surface composition

The XPS data enables evaluation of the carbon (C), oxygen (O), and nitrogen (N) surface ratios, it allows distinguishing the functional groups (chemical components) on the surface with and without fat samples. The O and N compositions are higher for the samples subjected to lipid extraction, samples M2 and M3 showed similar C, O and N signals compared to M1 (Figure 5.1). The fat extracted samples were characterized by lower C atomic percentage (Figure 5.1), this confirms that lipids are mainly responsible for the C signal in XPS analysis.
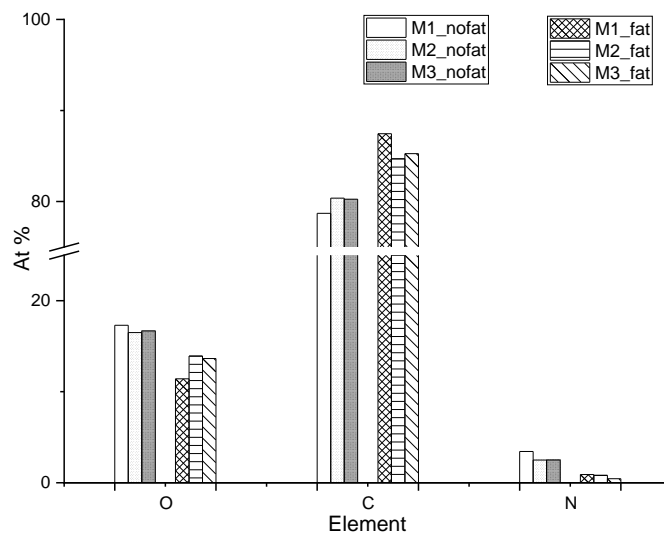
Figure 5.1. Plot depicting the surface compositional differences for extracted and non-extracted samples from the XPS analysis spectra.

The high-resolution spectra for carbon and oxygen signals are displayed in Figure 5.2, the signal intensities suggest surface heterogeneity among the samples. The carbon signal is attributed to the chemical species: $C–H_2$, C–OH, and HO–C=O. Particularly for the sample with lipid extraction, additional chemical specie is indicated, N-C=O, which is associated with theobromine. The binding energies for the analysis and signals were reported by Briggs (1998).
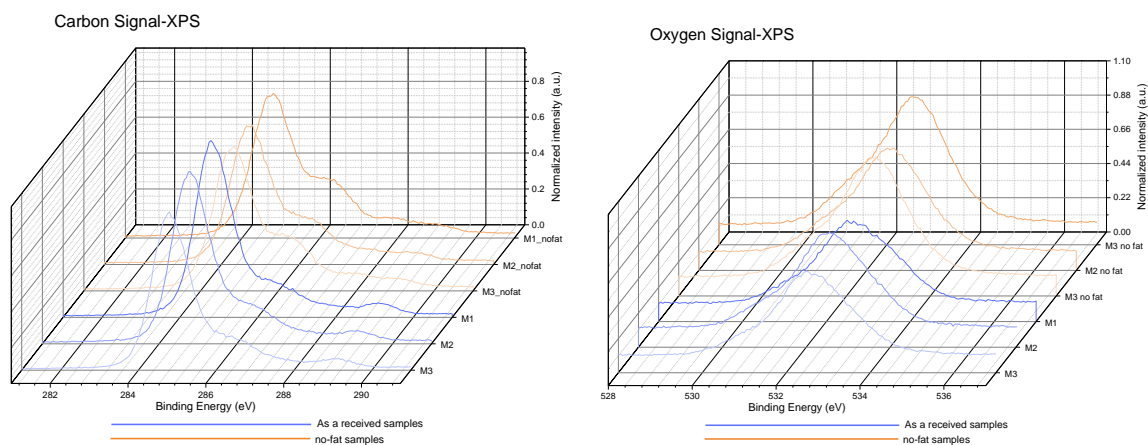

Figure 5.2. Illustrations of carbon and oxygen signals from the XPS analysis.

Conversely, the oxygen signals exhibit the presence of C=O and C–O–C for both groups of samples. However, the non-extracted samples display lower C–O–C signal intensities.

5.4.2   Surface phase transitions.

The IGC phase transition diagram (Figure 5.3) displays the Z-shape characteristic of a transition due to temperature. The regions A, B, and C show differences attributed to the interaction affinity between the adsorbent and the adsorbate. Without a transition, a straight line is obtained, and the behavior is predicted by Henry's law (Otte & Carvajal, 2011). Usually, in an amorphous system subjected to an increasing temperature ramp, the transition from the amorphous to the crystalline phase is characterized by the Z-shape diagram (Fernandez-Sanchez et al., 1991; Onjia & Nastasovi, 2008; Otte & Carvajal, 2011).
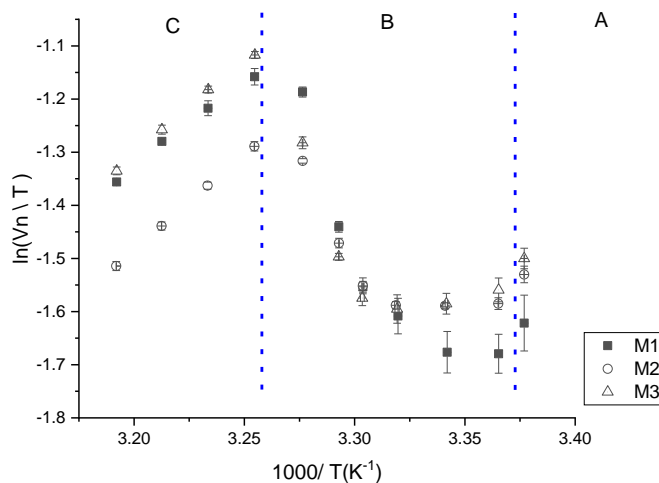
Figure 5.3. Phase transition diagram variations for cocoa powder extracted with *n*-heptane. The regions A, B, and C involve different phase transitions.

The Z-shape diagram for the glass transition temperature indicates that for region A, the adsorption equilibrium is at the surface. In region B, a non-equilibrium regime is at the edge of the surface and bulk location interface; whereas in region C, equilibrium is achieved by the bulk and

surface interactions (Onjia & Nastasovi, 2008). However, for a material with a defined crystalline phase, the equilibrium is mainly at the surface instead of the bulk (Otte & Carvajal, 2011). The latter is predominant in the cocoa samples because no glass transition temperature is detected by the differential scanning calorimetry (DSC). Melting-related phenomena are common for the entire temperature range due to the presence of polymorphs of various components (mainly lipids), rather than a single glass transition for a single component system. Additionally, the adsorbate retention volume can be described using the bulk and surface equilibrium interactions by the following equation (Onjia & Nastasovi, 2008):

$$V_g = K_a A_L + K_b V_L \qquad \text{Equation 5.11.}$$

where K_a is the surface adsorption partition coefficient, A_L is the surface area of the adsorbent, K_b is the bulk sorption partition coefficient, and V_L is the adsorbent volume. The K values, however, depend on the experimental conditions (Onjia & Nastasovi, 2008), and for our system, this variability was reduced by limiting equilibrium to the surfaces.

$$V_g = K_a A_L \qquad \text{Equation 5.12.}$$

The transitions in each region and the associated thermodynamics parameters are illustrated in Figure 5.4 for regions A and B and Figure 5.5 for region C.
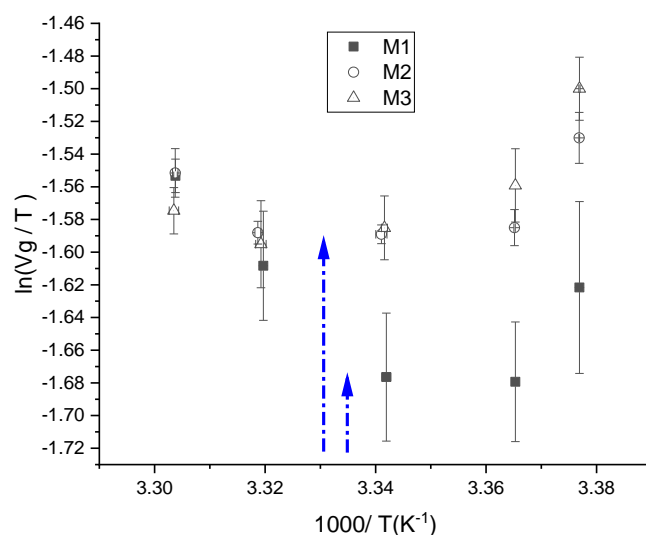
Figure 5.4. Retention diagram highlighting the transitions in regions A and B.

By analyzing the A region in Figure 5.4, the differences in the melting transition onset among the samples are apparent. The highest surface melting point is exhibited by M3, followed by M2 and M1. The IGC phase transition data for the surface presents different onset temperatures compared to those presented by the DSC data (chapters three and four). This also suggests that the surface thermal properties differ from the bulk.

Table 5.1. Cocoa transition temperatures measured by the IGC.

	T (°C)	SD
M1	24.64	0.58
M2	25.09	0.30
M3	25.68	0.07

The sintering, agglomeration and caking properties are driven by surface temperature variations and interactions. Therefore, information obtained by the IGC may serve in predicting the surface interaction mechanisms rather than the bulk thermal properties.
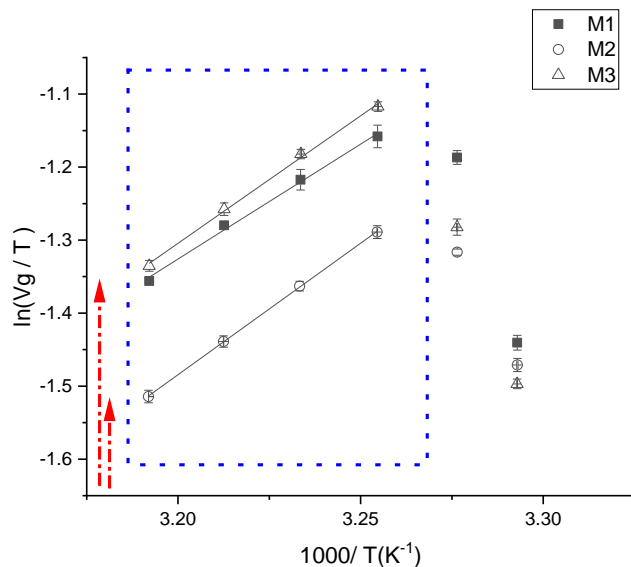
Figure 5.5. Retention diagram for the C region.

The sorption enthalpy of *n*-heptane in the cocoa powder was calculated in the C region of the retention diagram (Figure 5.5). Fernandez-Sanchez et al. (1991) suggested that if bulk and surface equilibriums are achieved in the C region, the enthalpy can be used to predict solubility. In our cocoa system, at the experimental temperature in the C region, the surface contains high proportions of energetic lipid polymorphs, and the surface equilibrium reflects the only possible interaction. The peaks of the raw retained *n*-heptane data confirm that only physisorption occurs, with symmetric peaks exhibited over the entire temperature range.

Table 5.2. Partial molar sorption enthalpies.

	ΔH (kJ/mol)	SD
M1	- 26.894	0.066
M2	- 27.338	0.226
M3	- 26.989	0.349

The molar enthalpy values of the cocoa powder in *n*-heptane range from −26 to −28 kJ/mol under isosteric conditions, thereby confirming that only physisorption occurs. Typically, for physisorption, the enthalpy (ΔH_s) range is from −4 to −40 kJ/mol, in contrast to chemisorption with values from −40 to −800 kJ/mol (Levine, 2009). The absolute enthalpy of sorption (ΔH_s) for M2 sample is the highest for among the samples, suggesting that the interaction between the adsorbent and adsorbate becomes stronger with increasing temperature. This information is useful for predicting the interphase stability, in addition to the blue and red arrows displayed in Figures 5.4 and 5.5, respectively. As displayed in Figure 5.4, the value for the M1 sample is initially low, but as the temperature increases in zone C, its value surpasses that of sample M2 in Figure 5.5. These differences are due to the surface interactions of the cocoa particles with the *n*-heptane. The lipid polymorphs with higher energetic properties are created when the temperature increases and the affinity between the cocoa particles and the *n*-heptane is altered. Further studies are needed to confirm this hypothesis. Experiments under different isosteric conditions as well as reducing the flow rate of the adsorbate would vary the magnitude of the interactions.

5.4.3 Activation energy of diffusion.

The water sorption isotherms were measured at 25, 30, 35 C to calculate the diffusion coefficients for the samples. Figure 5.6 shows the Arrhenius-type plots used for calculating the activation energy of diffusion. The plots show measurements at constant RH of 10% (Fig. 5.6 A) and 80% (Figure 5.6 B). The reason for choosing these RH values is that the R^2 values at other RH

values were significantly low, and these may favor a non-Arrhenius-type rate of diffusion. In fact, Chvoj et al. (1999) also explained the principle of non-Arrhenius diffusion coefficient behavior.
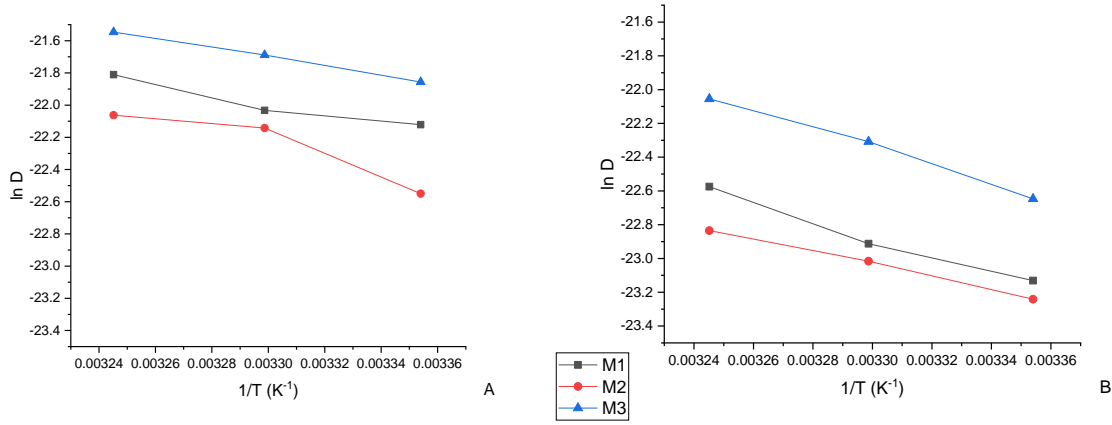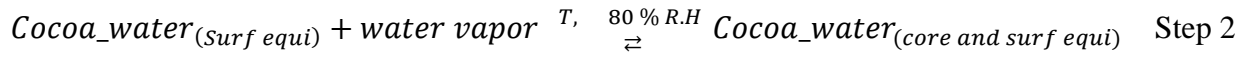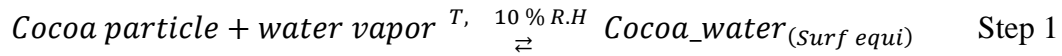

Figure 5.6. Arrhenius-type plots showing the relationships between the natural logarithm of the diffusion coefficient and temperature for (A)sorption data at 10% RH and (B) sorption data at 80% RH.

To explain the activation energy of diffusion, the sorption process is schematized following the chemical reaction analogy as follows:

$$Cocoa\ particle + water\ vapor \overset{T,\quad 10\ \%\ R.H}{\rightleftarrows} Cocoa\_water_{(Surf\ equi)} \qquad \text{Step 1}$$

$$Cocoa\_water_{(Surf\ equi)} + water\ vapor \overset{T,\quad 80\ \%\ R.H}{\rightleftarrows} Cocoa\_water_{(core\ and\ surf\ equi)} \qquad \text{Step 2}$$

First, the cocoa particles are exposed to water vapor at 10% RH; the products of this system are cocoa particles containing water in equilibrium with the surface. Second, when the RH is increased to 80%, the products are cocoa particles with water at the surface and core levels. This two-step process is reversible as indicated by the double arrows and it obeys the Le Chatelier's principle. Evidently, any change in the RH or cocoa particles disrupts the system equilibrium. The active energy barrier (Chvoj et al., 1999), for our purpose, can be called the activation energy of

diffusion, E_{ad}, and this is essentially constant for the temperature range evaluated (25–35 °C), as shown by the values in Table 5.3.

Table 5.3. The activation energy of diffusion in the cocoa system.

	10% RH		80% RH	
	Activation energy of diffusion (kJ/mol)	R^2	Activation energy of diffusion (kJ/mol)	R^2
M1	23.67	0.9382	42.45	0.9826
M2	37.33	0.8749	31.05	0.9971
M3	23.68	0.9984	45.28	0.9945

Regardless of the material, the activation energy of diffusion (E_{ad}) values are lower at 10% RH. According to chemical reaction interpretation (step 1 and 2), the low E_{ad} value implies that the diffusion process is faster at 10% RH that at 80%. This indicates that the sample susceptibility to water decreases as the relative humidity increases for samples M1 and M3. Interestingly, the shape of the sorption isotherms at different temperatures exhibit a pattern, as depicted in Figure 4.8a. For the 10 % RH plot, the diffusion coefficient increases considerably until it attains a maximum at around 40% RH. Conversely, for the plot at 80% RH, a steady state is already reached, and the water diffusion coefficients are minimum at RH between 60% and 90%. Therefore, the water migration mechanism proposed in chapter four is reinforced by the of activation energy values. Additionally, the M2 sample shows the lowest activation energy value at 80% RH and the highest value at 10%. This also suggests that the internal structure of this powder exhibits higher affinity for water than its surface. Further, the higher value at 10% RH for sample M2 may indicate

a high energy barrier that prevents water absorption into the powder. Improved stability to water is observed for the M2 sample at 10% RH, whereas this occurs for the M1 and M3 samples at 80% RH. The highest stability to temperature and water diffusion changes is therefore, predicted for the M2 sample.

5.5   Conclusions

The thermodynamic parameters for cocoa powder systems were evaluated by developing testing methods involving the IGC and DVS. The extent and degree of changes in the sorption enthalpy and activation energy of diffusion improved the understanding of the thermal and water interactions properties of these systems. Although studies using these parameters for food systems are scant, insightful relationships were obtained for the powders in this study. Physisorption was the primary mechanism for evaluating the thermodynamic properties using the IGC data. For cocoa, the gas probe–adsorbate equilibrium was achieved under isosteric conditions.

The methodology developed from these techniques was used for the first time to demonstrate phase transition and obtain the sorption enthalpy and Arrhenius energy of diffusion of cocoa-based systems. These results highlight the suitability of these techniques for food powders. Also, the methods developed herein may be used for experiments needed to examine the phase transition at different surface coverages. This work successfully evaluated the feasibility of the thermodynamics and surface approaches to address and improve physical attributes of complex food powdered systems such as cocoa.

5.6   References

Burgain, J., Petit, J., Scher, J., Rasch, R., Bhandari, B., & Gaiani, C. (2017). Progress in Surface Science Surface chemistry and microscopy of food powders. Progress in Surface Science, 92(4), 409-429.

Briggs, D. (1998). Surface analysis of polymers by XPS and static SIMS (Cambridge solid state science series). Chapter 3, Cambridge, U.K; New York: Cambridge University Press.

Chvoj. Z., Conrad. H., Chab, V. (1999). Analysis of the Arrhenius shape of adatom di ff usion coe ffi cient in a surface model with two energy barriers. 442, 455-462.

Fairley, N. (2009). CasaXPS Manual 2.3.15 Introduction to XPS and AES. Casa Software Ltd.

Fernandez-Sanchez E.F., Fernandez-Torres, A., Garcia-Dominguez, A.J., Salvador-Moya D. M. (1991). Gas chromatographic comparative study of superox 20M immobilized in different ways. Journal of Chromatography, 556 (1991) 485-493.

Fiorentini, C., Demarchi, S., Quintero, N., & Giner, S. (2015). ScienceDirect Arrhenius activation energy for water diffusion during drying of tomato leathers : The concept of characteristic product temperature. 2(1900), 1-8.

Jacquot, C., Petit, J., Michaux, F., Montes, E., Dupas, J., Girard, V., . . . Gaiani, C. (2016). Cocoa powder surface composition during aging : A focus on fat. *Powder Technology, 292*, 195-202.

Kovalenko, O., Vasiliev, S., & Tkatch, V. (2019). Correlation between parameters of Arrhenius-type temperature dependency for e ffctive diffusivity governing glass crystallization. Journal of Non-Crystalline Solids, 518, 36-42.

Laidler, K. J. (1972). Unconventional Applications of the Arrhenius Law. Journal of Chemical Education. 49, 5, 343-344.

Levine, I. (2009). Physical chemistry (6th ed.). Boston: McGraw-Hill.

Mitchell, W., Forny, L., Althaus, T., Niederreiter, G., Palzer, S., Hounslow, M., & Salman, A. (2019). Chemical Engineering Research and Design Surface tension-driven effects in the reconstitution of food powders. Chemical Engineering Research and Design, 146(1993), 464-469.

Murrieta-pazos, I., Gaiani, C., Galet, L., Calvet, R., Cuq, B., & Scher, J. (2012). Food powders : Surface and form characterization revisited. Journal of Food Engineering, 112(1-2), 1-21.

Onjia, A., & Nastasovi, A. (2008). Determination of glass temperature of polymers by inverse gas chromatography. 1195, 1-15.

Otte, A., & Carvajal, M. (2011). Assessment of Milling-Induced Disorder of Two Pharmaceutical Compounds. Journal of Pharmaceutical Sciences, 100(5), 1793-1804.

Selamat, J., Hussin, N., Zain, A., & Man, Y. (1998). Effects of alkalized cocoa powder and soy lecithin on physical characteristics of chocolate beverage powders. Journal of Food Processing and Preservation, *22*, 241-254.

VITA

Hector Lozano Perez was born on May 3, 1992 in Tunja, a town in the Boyaca state of Colombia. He attended to a countryside High School located in Sogamoso, Boyaca, Colegio Tecnico Gustavo Jimenez. He started his college studies at Universidad Nacional de Colombia in 2010. He graduated with Pharmaceutical Science bachelor's degree in 2016. In summer and fall 2015, he was a visiting scholar at Purdue University in the department of Agriculture and Biological Engineering. He worked as a quality assurance inspector in a Pharmaceutical Company in Colombia in 2017.

In spring 2018, Hector joined the Department of Agricultural and Biological Engineering at Purdue University as a graduate student. Hector holds a scholarship from Colfuturo, United States Agency for International Development (USAID) and the United States Department of Agriculture (USDA) agreement-scholarship. He is also a recipient of complementary financial aid from the Dane O. Kildsig Center of Pharmaceutical Processing and Research (CPPR). He served as teaching assistant of ABE 304 Bioprocess Engineering Laboratory in spring 2019 and interim laboratory manager in the Center for Particulate Products and Processes (CP3) at Purdue University, in summer and fall 2019.